Synthesis and Structural Characterization of Nonplanar Tetraphenylporphyrins and Their Metal Complexes with Graded Degrees of β-Ethyl Substitution

ARTICLE *in* INORGANIC CHEMISTRY · JANUARY 1998

Impact Factor: 4.76 · DOI: 10.1021/ic970765g · Source: PubMed

2 AUTHORS, INCLUDING:

Mathias O. Senge
Trinity College Dublin
375 PUBLICATIONS **5,920** CITATIONS

Synthesis and Structural Characterization of Nonplanar Tetraphenylporphyrins and Their Metal Complexes with Graded Degrees of β-Ethyl Substitution

Mathias O. Senge* and Werner W. Kalisch

Institut für Organische Chemie (WE02), Freie Universität Berlin, Takustrasse 3, D-14195 Berlin, Germany

Received June 19, 1997[⊗]

Different porphyrin conformations are believed to play a role in controlling the cofactor properties in natural tetrapyrrole−protein complexes. In order to study the correlation between macrocycle nonplanarity and physicochemical properties in detail, a series of six porphyrins with graded degrees of macrocycle distortion were synthesized via mixed condensation of pyrrole, diethylpyrrole, and benzaldehyde. The formal introduction of successively more β-ethyl groups into the tetraphenylporphyrin parent macrocycle gave access to diethyltetraphenylporphyrin (H_2DETPP), two regioisomers of tetraethyltetraphenylporphyrin (H_2tTETPP, H_2cTETPP), and hexaethyltetraphenylporphyrin (H_2HETPP). These conformationally designed compounds bridge the gap between the well-known tetraphenylporphyrin (H_2TPP) and the very nonplanar octaethyltetraphenylporphyrin (H_2OETPP), which are also formed during the reaction. Crystallographic studies showed that the macrocycle distortion in the solid state increases gradually in the order TPP < DETPP < tTETPP < cTETPP < HETPP < OETPP, i.e. with increasing degree of β-ethyl substitution and the number and localization of potential β-ethyl meso-phenyl interactions. This correlates well with increasing bathochromic shifts of the absorption bands in solution. Depending on the substituent pattern, different saddle-shaped macrocycle conformations were observed. While the conformation of tTETPP was symmetric, DETPP, cTETPP, and HETPP showed asymmetric distortion modes with individual β-pyrrole displacements reaching those described for dodecasubstituted porphyrins. Overall, higher displacements from planarity were found close to β-ethyl−meso-phenyl groups whereas smaller displacements were observed in parts of the molecules bearing β-hydrogen atoms. Nevertheless, a certain amount of redistribution of steric strain occurs as evidenced by significant displacements for pyrrole carbon atoms with β-hydrogens. Synthesis and structural investigation of the respective metal complexes with M = Cu(II), Ni(II), and Zn(II) showed similar correlations between β-ethyl substitution, bathochromic shift of absorption bands and nonplanarity as described for the free bases. The only exception was found for Ni^{II}tTETPP, which exhibited a highly nonplanar ruffled conformation. Additionally, the metal complexes allowed a study of the conformational effects of different metals at each level of macrocycle distortion. As observed for symmetric, nonplanar porphyrins larger metals led to a decrease in conformational distortion with associated changes in bond lengths and bond angles.

Introduction

Porphyrins with nonplanar macrocycle conformations have attracted considerable attention in recent years.[1] This is due to the hypothesis that fine-tuning of the macrocycle conformation by the protein scaffold is one way by which nature might control the physicochemical properties of the cofactors in intact tetrapyrrole−protein complexes.[2] This would account for the often quite different functions of the same chromophore when bound to different apoproteins. Indeed, more and more nonplanar tetrapyrrole macrocycle conformations are being identified in porphyrin−protein complexes.[1,3] In order to prepare suitable model compounds with nonplanar conformations, highly substituted porphyrins[4] have been utilized where steric congestion at the porphyrin periphery leads to distorted macrocycles.

A considerable body of information has now accumulated for such sterically overloaded porphyrins. The most prominent examples are 2,3,7,8,12,13,17,18-octaalkyl-5,10,15,20-tetraarylporphyrins,[2b,5−10] dodecaphenylporphyrin (H_2DPP),[11] 2,3,7,8,-12,13,17,18-octaethyl-5,10,15,20-tetranitroporphyrin,[12] and 2,3,7,8,12,13,17,18-octahalo-5,10,15,20-tetraarylporphyrins.[13] Due to their symmetry, these porphyrins are easily prepared via simple condensation reactions and mostly show highly nonplanar

* Corresponding author. E-mail: mosenge@chemie.fu-berlin.de.

⊗ Abstract published in *Advance ACS Abstracts,* December 1, 1997.

(1) (a) Fajer, J. *Chem. Ind.* (*London*) **1991**, 869. (b) Senge, M. O. *J. Photochem. Photobiol. B*: *Biol.* **1992**, *16*, 3. (c) Ravikanth, M.; Chandrashekar, T. K. *Struct. Bonding* (*Berlin*) **1995**, *82*, 105.

(2) (a) Forman, A.; Renner, M. W.; Fujita, E.; Barkigia, K. M.; Evans, M. C. W.; Smith, K. M.; Fajer, J. *Isr. J. Chem.* **1989**, *29*, 57. Gudowska-Nowak, E.; Newton, M. D.; Fajer, J. *J. Phys. Chem.* **1990**, *94*, 5795. Thompson, M. A.; Zerner, M. C.; Fajer, J. *J. Phys. Chem.* **1991**, *95*, 5693. (b) Barkigia, K. M.; Chantranupong, L.; Smith, K. M.; Fajer, J. *J. Am. Chem. Soc.* **1988**, *110*, 7566. (c) Huber, R. *Eur. J. Biochem.* **1990**, *187*, 283.

(3) Tronrud, D. E.; Schmid, M. F.; Matthews, B. W. *J. Mol. Biol.* **1986**, *188*, 443. Ermler, V.; Fritch, G.; Buchanan, S. K.; Michel, H. *Structure* **1994**, *2*, 925. Kühlbrandt, W.; Wang, D. N.; Fujiyoshi, Y. *Nature* **1994**, *367*, 614. Deisenhofer, J.; Epp, O.; Sinning, L.; Michel, H. *J. Mol. Biol.* **1995**, *246*, 429. Crane, B. R.; Siegl, L. M. L.; Getzoff, E. D. *Science* **1995**, *270*, 59. Hobbs, J. D.; Shelnutt, J. A. *J. Protein Chem.* **1995**, *14*, 19. McDermott, G.; Prince, S. M.; Freer, A. A.; Hawthornwaite-Lawless, A. M.; Papiz, M. Z.; Cogdell, R. J.; Isaacs, N. W. *Nature* **1995**, *374*, 517. Freer, A.; Prince, S.; Sauer, K., Papaz, M.; Hawthornwaite-Lawless, A.; McDermott, G.; Cogdell, R.; Isaacs, N. W. *Structure* **1996**, *4*, 449. Sauer, K.; Cogdell, R. J.; Prince, S. M.; Freer, A.; Isaacs, N. W.; Scheer, H. *Photochem. Photobiol.* **1996**, *64*, 564.

(4) Dolphin, D. *J. Heterocycl. Chem.* **1970**, *7*, 275. Hursthouse, M. B.; Neidle, S. *J. Chem. Soc., Chem. Commun.* **1972**, 449. Fuhrhop, J.-H.; Witte, L.; Sheldrick, W. S. *Liebigs Ann. Chem.* **1976**, 1537.

(5) (a) Medforth, C. J.; Berber, M. D.; Smith, K. M.; Shelnutt, J. A. *Tetrahedron Lett.* **1990**, *31*, 3719. (b) Shelnutt, J. A.; Medforth, C. J.; Berber, M. D.; Barkigia, K. M.; Smith, K. M. *J. Am. Chem. Soc.* **1991**, *113*, 4077. Sparks, L. D.; Anderson, K. K.; Medforth, C. J.; Smith, K. M.; Shelnutt, J. A. *Inorg. Chem.* **1994**, *33*, 2297. Medforth, C. J.; Hobbs, J. D.; Rodriguez, M. R.; Abraham, R. J.; Smith, K. M.; Shelnutt, J. A. *Inorg. Chem.* **1995**, *34*, 1333. (c) Senge, M. O.; Medforth, C. J.; Sparks, L. D.; Shelnutt, J. A.; Smith, K. M. *Inorg. Chem.* **1993**, *32*, 1716.

S0020-1669(97)00765-9 CCC: $14.00

saddle-shaped macrocycle conformations.[14] Ruffled conformations can be induced either by metal effects or via bulky meso-alkyl substituents[11b,15] while "dome-"[12b] or "wave-" type[11c,13b] distortion modes are found less frequently. In this context, 2,3,7,8,12,13,17,18-octaethyl-5,10,15,20-tetraphenylporphyrin (H_2OETPP), the structural hybrid of the planar octaethylporphyrin (H_2OEP) and tetraphenylporphyrin (H_2TPP), has become a kind of standard nonplanar porphyrin of choice and has been employed for a variety of physical, theoretical, and spectroscopic studies on porphyrin nonplanarity.[5b,10]

Nevertheless, several important questions remain to be addressed. Naturally occurring pigments have asymmetric substituent patterns and show distortions smaller than those observed in highly nonplanar dodecasubstituted porphyrins. Thus, a more detailed investigation of asymmetrically substituted porphyrins with various degrees of conformational distortion seemed advisable. In addition, most physicochemical studies on nonplanar porphyrins have studied all-or-nothing effects, e.g. by comparing a planar porphyrin like H_2TPP or H_2OEP with a very nonplanar porphyrin like H_2OETPP. In order to aid in the interpretation of the physicochemical data, rationally planned series of closely related porphyrins with different degree of macrocycle distortion are necessary. While some attempts have been made in this direction,[5,13b,16,17] either related planar compounds are not available for comparison or only fragmentary structural data have yet been published.

Therefore, we have embarked on a comprehensive study of asymmetrically substituted porphyrins and prepared a series of porphyrins with graded degrees of distortion in order to study the effect of different substituent patterns on the conformation. This should allow a more detailed correlation of the relationship between conformational distortion and (photo)physical properties. In light of the wealth of structural and physicochemical data available for the sterically unhindered H_2TPP and H_2OEP and now for the nonplanar H_2OETPP, a porphyrin series of choice seemed accessible via synthesis of ethyl-substituted tetraphenylporphyrins with intermediate degree of β-ethyl-substituted pyrrole rings closing the "conformational gap" between H_2TPP and H_2OETPP. This would give a series of six closely related porphyrins providing enough data points for a more detailed analysis. While preliminary results on the synthesis of the porphyrins have been reported in a communication,[18] we report here on the synthesis and properties of the free bases and metal complexes and give detailed structural information from crystal structure determinations for all compounds.

Experimental Section

General Procedures. Melting points were measured with a Reichert Thermovar instrument and are uncorrected. ^{1}H-NMR spectra were obtained in deuteriochloroform at 270 or 500 MHz using a Bruker AM 270 or AMX 500 spectrometer; chemical shifts are expressed in ppm relative to tetramethylsilane. Elemental analyses were performed on a Perkin-Elmer 240 elemental analyzer. Electronic absorption spectra were recorded on a UV/vis Specord S10 (Carl Zeiss) using dichloromethane for the metal complexes, dichloromethane with 1% triethylamine for the free bases, and dichloromethane with 1% TFA for the dications as solvents. Mass spectra were measured on a Varian MAT 711 spectrometer. Purification of the metal complexes were performed by using either silica gel 60 or Brockmann grade III basic alumina. Reactions were monitored by analytical TLC using precoated stripes of ALOX 60 or silica gel 60 plates.

Mixed Synthesis of H_2TPP, H_2DETPP, H_2tTETPP, H_2cTETPP, H_2HETPP, and H_2OETPP. A 1.34 g (0.02 mol) quantity of pyrrole, 2.46 g (0.02 mol) of diethylpyrrole, 4.24 g (0.04 mol) of benzaldehyde, and 0.5 mL (0.004 mol) of BF_3·OEt_2 were added to a 2 L round-bottom flask charged with 2 L of dry dichloromethane, and the reaction mixture was stirred for 12 h under argon. A 9.2 g (0.04 mol) quantity of DDQ was added all at once, and the solution was stirred for 1 h.

(6) (a) Evans, B.; Smith, K. M.; Fuhrhop, J.-H. *Tetrahedron Lett.* **1977**, *5*, 443. (b) Renner, M. W.; Barkigia, K. M.; Zhang, Y.; Medforth, C. J.; Smith, K. M.; Fajer, J. *J. Am. Chem. Soc.* **1994**, *116*, 8582. Medforth, C. J.; Muzzi, C. M.; Smith, K. M.; Abraham, R. J.; Hobbs, J. D.; Shelnutt, J. A., *J. Chem. Soc., Chem. Commun.* **1994**, 1843. Senge, M. O.; Forsyth, T. P.; Nguyen, L. T.; Smith, K. M. *Angew. Chem., Int. Ed. Engl.* **1994**, *33*, 2485. Renner, M. W.; Barkigia, K. M.; Melamed, D.; Smith, K. M.; Fajer, J. *Inorg. Chem.* **1996**, *35*, 5120. Cheng, R.-J.; Chen, P.-Y.; Gau, P.-R.; Peng, S.-M. *J. Am. Chem. Soc.* **1997**, *119*, 2563.

(7) Barkigia, K. M.; Berber, M. D.; Fajer, J.; Medforth, C. J.; Renner, M. W.; Smith, K. M. *J. Am. Chem. Soc.* **1990**, *112*, 8851.

(8) Sparks, L. D.; Medforth, C. J.; Park, M.-S.; Chamberlain, J.-R.; Ondrias, M. R.; Senge, M. O.; Smith, K. M.; Shelnutt, J. A. *J. Am. Chem. Soc.* **1993**, *115*, 581.

(9) Barkigia, K. M.; Renner, M. W.; Furenlid, L. R.; Medforth, C. J.; Smith, K. M.; Fajer, J. *J. Am. Chem. Soc.* **1993**, *115*, 3627.

(10) (a) Regev, A.; Galili, T.; Medforth, C. J.; Smith, K. M.; Barkigia, K. M.; Fajer, J.; Levanon, H. *J. Phys. Chem.* **1994**, *98*, 2520. (b) Charlesworth, P.; Truscott, T. G.; Kessel, D.; Medforth, C. J.; Smith, K. M. *J. Chem. Soc., Faraday Trans.* **1994**, *90*, 1073. Shelnutt, J. A.; Majumder, S. A.; Sparks, L. D.; Hobbs, J. D.; Medforth, C. J.; Senge, M. O.; Smith, K. M.; Miura, M.; Luo, L.; Quirke, J. M. E. *J. Raman Spectrosc.* **1992**, *23*, 523. Kadish, K. M.; Van Caemelbecke, E.; Boulas, P.; D'Souza, F.; Vogel, E.; Kisters, M.; Medforth, C. J.; Smith, K. M. *Inorg. Chem.* **1993**, *32*, 4177. Stichternath, A.; Schweitzer-Stenner, R.; Dreybrodt, W.; Mak, R. S. W.; Li, X.-y.; Sparks, L. D.; Shelnutt, J. A.; Medforth, C. J.; Smith, K. M. *J. Phys. Chem.* **1993**, *97*, 3701. Choi, S.; Philips, J. A.; Ware, W., Jr.; Wittschieben, C.; Medforth, C. J.; Smith, K. M. *Inorg. Chem.* **1994**, *33*, 3873. Gentemann, S.; Medforth, C. J.; Forsyth, T. P.; Nurco, D. J.; Smith, K. M.; Fajer, J.; Holten, D. *J. Am. Chem. Soc.* **1994**, *116*, 7363. Kadish, K. M.; Van Caemelbecke, E.; D'Souza, F.; Medforth, C. J.; Smith, K. M.; Tabard, A.; Guilard, R. *Organometallics* **1993**, *12*, 2411; *Inorg. Chem.* **1995**, *34*, 2984. Gentemann, S.; Nelson, N. Y.; Jaquinod, L.; Nurco, D. J.; Leung, S. H.; Medforth, C. J.; Smith, K. M.; Fajer, J.; Holten, D. *J. Phys. Chem. B* **1997**, *101*, 1247. Vitols, S. E.; Roman, J. S.; Ryan, D. E.; Blackwood, M. E., Jr.; Spiro, T. G. *Inorg. Chem.* **1997**, *36*, 764. Sibilia, S. A.; Hu, S.; Piffat, C.; Melamed, D.; Spiro, T. G. *Inorg. Chem.* **1997**, *36*, 1013.

(11) (a) Tsuchiya, S. *Chem. Phys. Lett.* **1990**, *169*, 608; *J. Chem. Soc., Chem. Commun.* **1992**, 1475. Medforth, C. J.; Smith, K. M. *Tetrahedron Lett.* **1990**, *31*, 5583. Takeda, J.; Ohya, T.; Sato, M. *Inorg. Chem.* **1992**, *31*, 2877. Takeda, J.; Sato, M. *Chem. Lett.* **1995**, 939, 971. (b) Medforth, C. J.; Senge, M. O.; Smith, K. M.; Sparks, L. D.; Shelnutt, J. A. *J. Am. Chem. Soc.* **1992**, *114*, 9859. (c) Nurco, D. J.; Medforth, C. J.; Forsyth, T. P.; Olmstead, M. M.; Smith, K. M. *J. Am. Chem. Soc.* **1996**, *118*, 10918.

(12) (a) Gong, L.-C.; Dolphin, D. *Can. J. Chem.* **1985**, *63*, 401. Wu, G.-Z.; Gan, W.-X.; Leung, H.-K. *J. Chem. Soc., Faraday Trans.* **1991**, *87*, 2933. Hobbs, J. D.; Majumder, S. A.; Luo, L.; Sickelsmith, G. A.; Quirke, J. M. W.; Medforth, C. J.; Smith, K. M.; Shelnutt, J. A. *J. Am. Chem. Soc.* **1994**, *116*, 3261. Senge, M. O.; Smith, K. M. *J. Chem. Soc., Chem. Commun.* **1994**, 923. (b) Senge, M. O. *J. Chem. Soc., Dalton Trans.* **1993**, 3539.

(13) (a) Bhyrappa, P.; Krishnan, V. *Inorg. Chem.* **1991**, *20*, 239. Mandon, D.; Ochsenbein, P.; Fischer, J.; Weiss, R.; Jayaraj, K.; Austin, R. N.; Gold, A.; White, P. S.; Brigaud, O.; Battioni, P.; Mansuy, D. *Inorg. Chem.* **1992**, *31*, 2044. Henling, L. M.; Schaefer, W. P.; Hodge, J. A.; Hughes, M. E.; Gray, H. B. *Acta Crystallogr.* **1993**, *C49*, 1743. Bhyrappa, P.; Nethaji, M.; Krishnan, V. *Chem. Lett.* **1993**, 869. Bhyrappa, P.; Krishnan, V.; Nethaji, M. *J. Chem. Soc., Dalton Trans.* **1993**, 1901. Ochsenbein, P.; Mandon, D.; Fischer, J.; Weiss, R.; Austin, R.; Jayaraj, K.; Gold, A.; Terner, J.; Bill, E.; Müther, M.; Trautwein, A. X. *Angew. Chem., Int. Ed. Engl.* **1993**, *32*, 1437. Birnbaum, E. R.; Hodge, J. A.; Grinstaff, M. W.; Schaefer, W. P.; Henling, L.; Labinger, J. A.; Bercaw, J. E.; Gray, H. B. *Inorg. Chem.* **1995**, *34*, 3625. (b) Ochsenbein, P.; Ayougou, K.; Mandon, D.; Fischer, J.; Weiss, R.; Austin, R. N.; Jayaraj, K.; Gold, A.; Terner, J.; Fajer, J. *Angew. Chem., Int. Ed. Engl.* **1994**, *33*, 348.

(14) For definitions of the different distortion modes see: Scheidt, W. R.; Lee, Y. J. *Struct. Bonding* (*Berlin*) **1987**, *64*, 1.

(15) (a) Ema, T.; Senge, M. O.; Nelson, N. Y.; Ogoshi, H.; Smith, K. M. *Angew. Chem., Int. Ed. Engl.* **1994**, *33*, 1879. (b) Senge, M. O.; Ema, T.; Smith, K. M. *J. Chem. Soc., Chem. Commun.* **1995**, 733.

(16) Takeda, J.; Sato, M. *Tetrahedron Lett.* **1994**, *35*, 3565; *Chem. Lett.* **1994**, 2233.

(17) Chan, K. S.; Zhou, X.; Luo, B.-s.; Mak, T. C. W. *J. Chem. Soc., Chem. Commun.* **1994**, 271.

(18) Kalisch, W. W.; Senge, M. O. *Tetrahedron Lett.* **1996**, *37*, 1183.

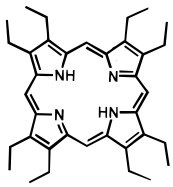

H_2OEP

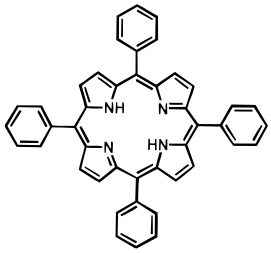

H_2TPP

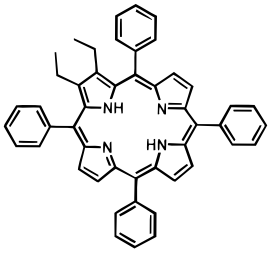

H_2DETPP

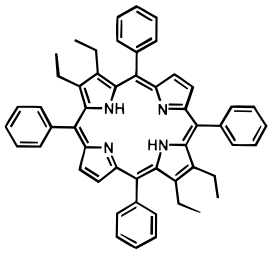

H_2tTETPP

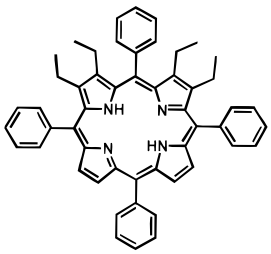

H_2cTETPP

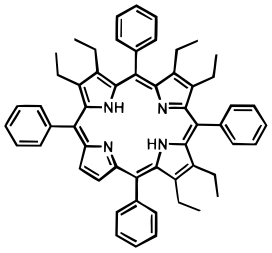

H_2HETPP

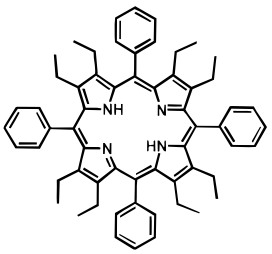

H_2OETPP

Subsequently, the reaction mixture was filtered through alumina followed by column chromatography on Brockmann grade III basic alumina using toluene with an increasing content of methanol as eluant. Three crude fractions were obtained which showed the following composition: (a) H_2TPP/H_2DETPP, (b) H_2tTETPP/H_2cTETPP, and (c) H_2HETPP/H_2OETPP. H_2TPP and H_2DETPP were separated on a silica gel column, eluting with toluene/hexane, 1/1 (v/v), while *trans*- and *cis*-TETPP could be separated using an alumina column, eluting with toluene containing 0.5% methanol. The third crude fraction, containing H_2HETPP and H_2OETPP, could not be separated directly. Thus, the free bases were converted into the corresponding iron(III) chloride derivatives and separated by column chromatography on alumina (toluene containing 1% NEt_3) followed by demetalation to the free bases. Alternatively and more conveniently, the H_2HETPP and H_2OETPP mixture could be converted to the respective Ni(II) complexes, which could then be separated via preparative HPLC using a silica gel column and 2% THF in hexane as eluant, followed by demetalation. Recrystallization of the individual fractions from dichloromethane/methanol yielded deep purple crystals: 1.12 g (16.8%) of H_2TPP, 0.97 g (14.4%) of H_2DETPP, 0.12 g (1.65%) of H_2tTETPP, 0.88 g (12.1%) of H_2cTETPP, 0.65 g (9.8%) of H_2HETPP, and 1.21 g (18.1%) of H_2OETPP.

2,3-Diethyl-5,10,15,20-tetraphenylporphyrin, H_2DETPP. Mp: 324−325 °C. UV/vis (CH_2Cl_2 + 1% NEt_3), λ_{max}, nm (log ϵ): 420 (5.62), 521 (4.27), 555 (3.74), 591 (3.81), 645 (3.53). UV/vis (CH_2Cl_2 + 1% TFA), λ_{max}, nm (log ϵ): 445 (5.61), 555 sh (3.79), 605 sh (4.09), 663 (4.67). ^{1}H-NMR (500 MHz, $CDCl_3$): δ −3.04 (br s, 1H, N*H*), −2.45 (br s, 1H, N*H*), 1.00 (t, ^3J = 7.5 Hz, 6H, CH_3), 2.85 (m, 4H, CH_2), 7.72 (m, 12H, H_{m-Ph}, H_{p-Ph}), 8.20 (m, 8H, H_{o-Ph}), 8.56 (d, ^3J = 5 Hz, 2H, $H_{pyrrole}$, 7-H, 18-H), 8.67 (d, ^3J = 5 Hz, 2H, $H_{pyrrole}$, 8-H, 17-H), 8.94 (s, 2H, $H_{pyrrole}$, 12-H, 13-H). MS, *m/z* (relative intensity, %): 670 (100) [M^+], 335 (12) [M^{2+}]. HRMS, *m/z*: calcd for $C_{48}H_{38}N_4$, 670.30965; found, 670.30926. Anal. Calcd for $C_{48}H_{38}N_4$: C, 85.94; H, 5.71; N, 8.35. Found: C, 85.77; H, 5.78; N, 8.18.

2,3,12,13-Tetraethyl-5,10,15,20-tetraphenylporphyrin, H_2tTETPP. Mp: 296−298 °C. UV/vis (CH_2Cl_2 + 1% NEt_3), λ_{max}, nm (log ϵ): 426 (5.47), 527 (4.17), 593 (3.70), 649 (3.32). UV/vis (CH_2Cl_2 + 1% TFA), λ_{max}, nm (log ϵ): 451 (5.55), 668 (4.58). ^{1}H-NMR (500 MHz, $CDCl_3$): δ −2.60 (s, 2H, N*H*), 0.86 (t, ^3J = 7.5 Hz, 12H, CH_3), 2.81 (q, ^3J = 7.5 Hz, 8H, CH_2), 7.66−7.78 (m, 12H, H_{m-Ph}, H_{p-Ph}), 8.21 (m, 8H, H_{o-Ph}), 8.30 (s, 4H, $H_{pyrrole}$). MS, *m/z* (relative intensity, %): 726 (100) [M^+], 698 (44), 363 (6) [M^{2+}]. HRMS, *m/z*: calcd for $C_{52}H_{46}N_4$, 726.372 25; found, 726.372 93. Anal. Calcd for $C_{52}H_{46}N_4 \cdot H_2O$: C, 83.84; H, 6.49; N, 7.52. Found: C, 83.80; H, 6.28; N, 7.24.

2,3,7,8-Tetraethyl-5,10,15,20-tetraphenylporphyrin, H_2cTETPP. Mp: 315−316 °C. UV/vis (CH_2Cl_2 + 1% NEt_3), λ_{max}, nm (log ϵ): 433 (5.38), 540 (4.15), 575 (3.92), 604 (3.82), 672 (3.63). UV/vis (CH_2Cl_2 + 1% TFA), λ_{max}, nm (log ϵ): 455 (5.55), 588 sh (3.52), 621 sh (3.90), 675 (4.67). ^{1}H-NMR (250 MHz, $CDCl_3$): δ −2.38 (br s, 2H, N*H*), 0.46 (m, 6H, CH_3), 0.68 (t, ^3J = 7.5 Hz, 6H, CH_3), 2.36 (br s, 4H, CH_2), 2.56 (br s, 4H, CH_2), 7.74 (m, 12H, H_{m-Ph}, H_{p-Ph}), 8.36 (m, 8H, H_{o-Ph}), 8.56 (s, 4H, $H_{pyrrole}$). MS, *m/z* (relative intensity, %): 726 (100) [M^+], 711 (10), 698 (44), 679 (11), 363 (15) [M^{2+}]. HRMS, *m/z*: calcd for $C_{52}H_{46}N_4$, 726.372 25; found, 726.372 11. Anal. Calcd for $C_{52}H_{46}N_4$: C, 85.92; H, 6.38; N, 7.71. Found: C, 85.88; H, 6.43; N, 7.53.

2,3,7,8,12,13-Hexaethyl-5,10,15,20-tetraphenylporphyrin, H_2HETPP. Mp: 295−297 °C. UV/vis (CH_2Cl_2 + 1% NEt_3), λ_{max}, nm (log ϵ): 444 (5.35), 544 (4.12), 588 (3.90), 623 (3.72), 685 (3.45). UV/vis (CH_2Cl_2 + 1% TFA), λ_{max}, nm (log ϵ): 462 (5.54), 570 sh (3.82), 525 sh (4.08), 683 (4.61). ^{1}H-NMR (250 MHz, $CDCl_3$): δ −2.23 (br s, 2H, N*H*), 0.35 (m, 6H, CH_3), 0.48 (m, 6H, CH_3), 0.66 (m, 6H, CH_3), 1.49 (m, 2H, CH_2), 2.15 (m, 4H, CH_2), 2.55 (m, 6H, CH_2), 7.65 (m, 12H, H_{m-Ph}, H_{p-Ph}), 8.25 (m, 10H, H_{o-Ph}, $H_{pyrrole}$). MS, *m/z* (relative intensity, %): 782 (100) [M^+], 392 (13) [M^{2+}]. HRMS, *m/z*: calcd for $C_{56}H_{54}N_4$, 782.434 85; found: 782.434 36. Anal. Calcd for $C_{56}H_{54}N_4 \cdot 0.5$MeOH: C, 84.92; H, 7.06; N, 7.01. Found: C, 84.78; H, 6.90; N, 6.81.

Metal Complexes. Most Zn, Ni, and Cu complexes were prepared from the corresponding free-base porphyrins using standard metal acetate methodology.[19] The preparation of **Zn^{II}cTETPP** and **Zn^{II}HETPP** could more easily be performed by the following method. E.g., 70 mg (0.09 mmol) of **H_2HETPP**, 200 mg (0.9 mmol) of anhydrous zinc bromide, and 330 mg of active potassium carbonate (2.4 mmol) were stirred in 2 mL of dry THF and 10 mL of dichloromethane for 30 min. After filtration, the solvent was removed in vacuo, the residue was dissolved again in dichloromethane with a trace of dry methanol, and the solution was filtered again. Recrystallization from dichloromethane/hexane under anhydrous conditions yielded 70 mg (0.08 mmol, 90%) of deep violet crystals of **Zn^{II}HETPP**.

(2,3-Diethyl-5,10,15,20-tetraphenylporphyrinato)zinc(II), Zn^{II}DETPP. Mp: >350 °C. UV/vis (CH_2Cl_2), λ_{max}, nm (log ϵ): 420 (5.71), 550 (4.33). ^{1}H-NMR (500 MHz, $CDCl_3$): δ 1.08 (t, ^3J = 7.5 Hz, 6H, CH_3), 2.82 (q, ^3J = 7.5 Hz, 4H, CH_2), 7.62−7.80 (m, 12H, H_{m-Ph}, H_{p-Ph}), 8.19 (m, 8H, H_{o-Ph}), 8.70 (d, ^3J = 6.5 Hz, 2H, $H_{pyrrole}$, 7-H, 18-H), 8.84 (d, ^3J = 6.5 Hz, 2H, $H_{pyrrole}$, 8-H, 17-H), 8.88 (s, 2H, $H_{pyrrole}$, 12-H, 13-H). MS, *m/z* (relative intensity, %): 732 (100) [M^+], 688 (20), 611 (34), 366 [M^{2+}]. Anal. Calcd for $C_{48}H_{36}N_4Zn$: C, 78.52; H, 4.94; N, 7.63. Found: C, 78.52; H, 5.05; N, 7.37.

(2,3,12,13-Tetraethyl-5,10,15,20-tetraphenylporphyrinato)zinc(II), Zn^{II}tTETPP. Mp: >350 °C. UV/vis (CH_2Cl_2), λ_{max}, nm (log ϵ): 424 (5.33), 554 (3.97). ^{1}H-NMR (500 MHz, $CDCl_3$): δ 0.93 (t, ^3J = 7.5 Hz, 12H, CH_3), 2.75 (q, ^3J = 7.5 Hz, 8H, CH_2), 7.66−7.76 (m,

(19) Smith, K. M., Ed. *Porphyrins and Metalloporphyrins*; Elsevier: Amsterdam, 1975.

Table 1. Crystal Data and Data Collection Parameters for the Compounds Studied

	H_2DETPP	H_2tTETPP	H_2cTETPP	H_2HETPP	Ni^{II}DETPP	Ni^{II}tTETPP
empirical formula	$C_{48}H_{38}N_4$	$C_{52}H_{46}N_4 \cdot CH_2Cl_2$	$C_{52}H_{46}N_4 \cdot 2CH_3OH$	$C_{56}H_{54}N_4 \cdot 1.3CH_2Cl_2$	$C_{48}H_{36}N_4Ni$	$C_{52}H_{44}N_4Ni$
crystal size, mm	1 × 0.58 × 0.52	0.25 × 0.25 × 0.19	0.2 × 0.18 × 0.12	0.6 × 0.6 × 0.2	0.44 × 0.3 × 0.08	0.36 × 0.24 × 0.16
color	red	blue	black	blue-black	red	red
habit	irregular shape	rhombus	block	irregular shape	plate	rhombus
mol wt	670.8	811.9	791.01	893.4	727.5	783.6
space group	*Cc*	$P2_1/c$	$P2_1/c$	$P2_1/c$	$P2_1/c$	*C*2
a, Å	18.333(12)	13.531(6)	16.992(5)	11.274(4)	13.198(9)	18.087(8)
b, Å	20.664(14)	28.172(11)	16.206(3)	17.186(7)	8.385(6)	12.239(3)
c, Å	10.180(6)	12.184(4)	17.247(6)	25.339(9)	29.227(9)	18.037(7)
α, deg	90	90	90	90	90	90
β, deg	109.65(5)	112.55(3)	115.66(2)	98.51(3)	90.72(4)	92.67(3)
γ, deg	90	90	90	90	90	90
V, Å^3	3632(4)	4289(3)	4281(2)	4856(3)	3479(4)	3989(3)
Z	4	4	4	4	4	4
D_{calcd}, g·cm^{-3}	1.227	1.257	1.227	1.222	1.389	1.305
μ, mm^{-1}	0.072	1.676	0.578	0.209	1.126	1.019
radiation	Mo Kα	Cu Kα	Cu Kα	Mo Kα	Cu Kα	Cu Kα
λ, Å	0.710 73	1.541 78	1.541 78	0.710 73	1.541 78	1.541 78
diffractometer	Siemens R3m/V	Syntex $P2_1$	Siemens P4/RA	Siemens R3m/V	Syntex $P2_1$	Siemens P4/RA
T, K	130	130	118	293	130	130
θ_{max}, deg	27.52	57.06	56.08	24	54.1	56.4
no. of indep reflns	4412	5796	5589	7616	4218	2778
no. of obs reflns	3664	3595	3948	4056	2841	2633
no. of params	469	366	542	578	311	347
R1 ($I > 2.0\sigma(I)$)[a]	0.052	0.116	0.068	0.086	0.087	0.062
wR2 ($I > 2.0\sigma(I)$)[b]	0.137	0.264	0.168	0.224	0.212	0.162
R1 (all data)[a]	0.067	0.175	0.101	0.162	0.128	0.066
wR2 (all data)[b]	0.160	0.309	0.195	0.290	0.245	0.170
S	0.792	1.053	1.05	1.026	1.037	0.959

	Ni^{II}cTETPP	Ni^{II}HETPP	Cu^{II}DETPP	Cu^{II}tTETPP	Cu^{II}cTETPP	Cu^{II}HETPP
empirical formula	$C_{52}H_{44}N_4Ni$	$C_{56}H_{52}N_4Ni$	$C_{48}H_{36}N_4Cu$	$C_{52}H_{44}N_4Cu \cdot CH_2Cl_2$	$C_{52}H_{44}N_4Cu$	$C_{56}H_{52}N_4Cu$
crystal size, mm	1 × 0.3 × 0.15	0.55 × 0.38 × 0.1	0.24 × 0.16 × 0.03	0.52 × 0.26 × 0.22	0.8 × 0.03 × 0.02	0.4 × 0.16 × 0.1
color	blue	red	red	red	red	black
habit	parallelepiped	parallelepiped	parallelepiped	parallelepiped	fiber	parallelepiped
mol wt	783.6	839.7	732.4	873.4	788.5	844.6
space group	$P\bar{1}$	$P\bar{1}$	$P\bar{1}$	$P\bar{1}$	$P\bar{1}$	$P\bar{1}$
a, Å	10.602(5)	12.735(3)	13.658(4)	12.321(3)	10.471(3)	12.826(7)
b, Å	13.112(7)	12.915(3)	14.279(4)	13.429(4)	13.201(3)	12.920(7)
c, Å	16.085(11)	14.007(3)	18.569(5)	13.679(4)	16.211(6)	14.207(7)
α, deg	113.53(4)	78.37(2)	92.68(2)	99.80(2)	113.74(2)	78.98(4)
β, deg	92.84(6)	68.89(2)	97.72(2)	94.14(2)	92.77(3)	69.02(4)
γ, deg	99.34(4)	83.84(2)	93.52(2)	105.83(2)	99.00(2)	84.49(5)
V, Å^3	2007(2)	2103.5(8)	3576(2)	2128.8(10)	2010.5(10)	2157(2)
Z	2	2	4 (2 indep mol)	2	2	2
D_{calcd}, g·cm^{-3}	1.297	1.326	1.360	1.363	1.302	1.301
μ, mm^{-1}	0.526	1.000	1.175	2.202	0.585	0.550
radiation	Mo Kα	Cu Kα	Cu Kα	Cu Kα	Mo Kα	Mo Kα
λ, Å	0.710 73	1.541 78	1.541 78	1.541 78	0.710 73	0.710 73
diffractometer	Siemens R3m/V	Syntex $P2_1$	Siemens P4/RA	Syntex $P2_1$	Siemens R3m/V	Siemens R3m/V
T, K	293	130	120	126	293	293
θ_{max}, deg	27.5	56.44	57.04	57.04	25	25
no. of indep reflns	9206	5643	9456	5753	7109	7578
no. of obs refls	5878	4603	7057	4479	4195	4333
no. of params	515	428	956	541	397	551
R1 ($I > 2.0\sigma(I)$)[a]	0.060	0.068	0.053	0.059	0.078	0.070
wR2 ($I > 2.0\sigma(I)$)[b]	0.146	0.172	0.121	0.139	0.171	0.130
R1 (all data)[a]	0.105	0.084	0.079	0.080	0.145	0.146
wR2 (all data)[b]	0.197	0.201	0.138	0.153	0.221	0.180
S	0.776	1.037	1.021	1.034	1.025	1.012

	Zn^{II}DETPP(*β*-pic)	Zn^{II}DETPP(MeOH)	Zn^{II}tTETPP(pyr)	Zn^{II}cTETPP(pyr)	Zn^{II}HETPP	Zn^{II}HETPP(pyr)
empirical formula	$C_{54}H_{43}N_5Zn$	$C_{49}H_{40}N_4OZn$	$C_{57}H_{49}N_5Zn \cdot 0.4H_2O$	$C_{57}H_{49}N_5Zn$	$C_{56}H_{52}N_4Zn$	$C_{61}H_{57}N_5Zn \cdot 2CH_2Cl_2$
crystal size, mm	0.4 × 0.4 × 0.4	0.43 × 0.4 × 0.04	0.75 × 0.3 × 0.22	0.8 × 0.4 × 0.3	0.83 × 0.43 × 0.25	0.8 × 0.7 × 0.6
color	red	red	red	red	red-black	blue-black
habit	cube	plate	parallelepiped	parallelepiped	irregular block	irregular block
mol wt	827.3	766.2	876.6	869.38	846.4	1095.3
space group	$P\bar{1}$	$P\bar{1}$	$P\bar{1}$	$P\bar{1}$	$P\bar{1}$	*Cc*
a, Å	10.033(2)	10.387(4)	12.800(4)	12.142(3)	12.736(3)	17.284(5)
b, Å	16.124(4)	10.808(5)	13.985(6)	13.794(4)	12.775(4)	21.509(6)
c, Å	16.447(5)	17.503(12)	14.152(5)	15.574(5)	14.214(3)	16.118(4)
α, deg	60.94(2)	92.19(5)	85.08(3)	69.06(3)	79.55(2)	90
β, deg	83.16(2)	95.88(4)	68.22(3)	72.05(2)	68.39(2)	111.55(2)
γ, deg	85.73(2)	97.81(3)	72.60(3)	69.93(2)	85.21(2)	90

Table 1 (Continued)

	Zn^{II}DETPP(β-pic)	Zn^{II}DETPP(MeOH)	Zn^{II}tTETPP(pyr)	Zn^{II}cTETPP(pyr)	Zn^{II}HETPP	Zn^{II}HETPP(pyr)
V, Å^3	2309(1)	1934(2)	2243.9(14)	2236.5(11)	2114.1(9)	5573(3)
Z	2	2	2	2	2	4
D_{calcd}, g·cm^{-3}	1.190	1.316	1.297	1.291	1.330	1.305
μ, mm^{-1}	0.572	1.212	1.108	0.594	1.140	0.677
radiation	Mo Kα	Cu Kα	Cu Kα	Mo Kα	Cu Kα	Mo Kα
λ, Å	0.710 73	1.541 78	1.541 78	0.710 73	1.541 78	0.710 73
diffractometer	Siemens R3m/V	Syntex $P2_1$	Syntex $P2_1$	Siemens R3m/V	Syntex $P2_1$	Siemens R3m/V
T, K	293	130	126	126	126	126
θ_{max}, deg	26	57.04	57.04	27.5	57.01	27.5
no. of indep reflns	9086	5217	6072	10282	6002	6610
no. of obs reflns	6565	3848	5075	6493	4046	6014
no. of params	542	497	560	568	413	658
R1 ($I > 2.0\sigma(I)$)[a]	0.068	0.083	0.060	0.062	0.064	0.045
wR2 ($I > 2.0\sigma(I)$)[b]	0.202	0.208	0.149	0.124	0.164	0.096
R1 (all data)[a]	0.097	0.111	0.073	0.119	0.068	0.038
wR2 (all data)[b]	0.257	0.234	0.162	0.157	0.167	0.088
S	0.819	1.024	1.028	1.017	1.044	1.020

[a] $R1 = \sum||F_o| - |F_c||/\sum|F_o|$. [b] $wR2 = [\sum(w(F_o^2 - F_c^2)^2)/\sum(w(F_o^2)^2)]^{1/2}$.

12H, H_{m-Ph}, H_{p-Ph}), 8.19 (m, 8H, H_{o-Ph}), 8.58 (s, 4H, $H_{pyrrole}$). MS, *m/z* (relative intensity, %): 788 (100) [M^+], 394 (12) [M^{2+}]. Anal. Calcd for $C_{52}H_{44}N_4Zn$: C, 79.03; H, 5.56; N, 7.09. Found: C, 78.75; H, 5.39; N, 6.78.

(2,3,7,8-Tetraethyl-5,10,15,20-tetraphenylporphyrinato)zinc-(II), Zn^{II}cTETPP. Mp: >350 °C. UV/vis (CH_2Cl_2), λ_{max}, nm (log ϵ): 431 (5.42), 561 (4.16), 611 sh (3.34). ^{1}H-NMR (500 MHz, $CDCl_3$): δ 0.58, 0.81 (each t, ^3J = 7.5 Hz, 12H, CH_3), 2.40, 2.67 (each q, ^3J = 7.5 Hz, 8H, CH_2), 7.66−7.85 (m, 12H, H_{m-Ph}, H_{p-Ph}), 8.17−8.39 (m, 8H, H_{o-Ph}), 8.63, 8.70 (each d, ^3J = 5 Hz, 4H, $H_{pyrrole}$). MS, *m/z* (relative intensity, %): 788 (100) [M^+], 715 (11), 394(13) [M^{2+}]. Anal. Calcd for $C_{52}H_{44}N_4Zn$·0.5MeOH: C, 78.20; H, 5.75; N, 6.95. Found: C, 78.26; H, 5.61; N, 6.81.

(2,3,7,8,12,13-Hexaethyl-5,10,15,20-tetraphenylporphyrinato)-zinc(II), Zn^{II}HETPP. Mp: > 330 °C. UV/vis (CH_2Cl_2), λ_{max}, nm (log ϵ): 443 (5.38), 572 (4.30). ^{1}H-NMR (250 MHz, $CDCl_3$): δ 0.49, 0.51, 0.71 (each t, ^3J = 7.5 Hz, 18H, CH_3), 2.35, 2.37, 2.61 (each q, ^3J = 7.5 Hz, 12H, CH_2), 7.62−7.85 (m, 12H, H_{m-Ph}, H_{p-Ph}), 8.21−8.43 (m, 8H, H_{o-Ph}), 8.46 (s, 2H, $H_{pyrrole}$). MS, *m/z* (relative intensity, %): 844 (100) [M^+], 422 (19) [M^{2+}]. Anal. Calcd for $C_{56}H_{52}N_4Zn$·H_2O: C, 77.81; H, 6.30; N, 6.48. Found: C, 77.60; H, 6.14; N, 6.24.

(2,3-Diethyl-5,10,15,20-tetraphenylporphyrinato)copper(II), Cu^{II}DETPP. Mp: 345 °C. UV/vis (CH_2Cl_2), λ_{max}, nm (log ϵ): 417 (5.61), 543 (4.28). MS, *m/z* (rel. int, %): 731 (100), [M^+], 657 (23), 609 (33), 365 (14) [M^{2+}]. Anal. Calcd for $C_{48}H_{36}N_4Cu$: C, 78.72; H, 4.95; N, 7.65. Found: C, 78.75; H, 5.12; N, 7.40.

(2,3,12,13-Tetraethyl-5,10,15,20-tetraphenylporphyrinato)copper-(II), Cu^{II}tTETPP. Mp: >350 °C. UV/vis (CH_2Cl_2), λ_{max}, nm (log ϵ): 422 (5.33), 552 (3.34). MS, *m/z* (rel. int, %): 787 (100) [M^+], 759 (19), 393 (7) [M^{2+}]. Anal. Calcd for $C_{52}H_{44}N_4Cu$: C, 79.21; H, 5.62; N, 7.11. Found: C, 79.38; H, 5.80; N, 6.71.

(2,3,7,8-Tetraethyl-5,10,15,20-tetraphenylporphyrinato)copper-(II), Cu^{II}cTETPP. Mp: >350 °C. UV/vis (CH_2Cl_2), λ_{max}, nm (log ϵ): 424 (5.47), 548 (4.43), 562 sh (3.35). MS, *m/z* (relative intensity, %): 787 (100) [M^+], 393 (22) [M^{2+}]. Anal. Calcd for $C_{52}H_{44}N_4Cu$: C, 79.21; H, 5.62; N, 7.11. Found: C, 79.32; H, 5.81; N, 6.87.

(2,3,7,8,12,13-Hexaethyl-5,10,15,20-tetraphenylporphyrinato)copper(II), Cu^{II}HETPP. Mp: >350 °C. UV/vis (CH_2Cl_2), λ_{max}, nm (log ϵ): 429 (5.45), 547(4.45), 566 (4.49). MS, *m/z* (relative intensity, %): 843 (100) [M^+], 421 (19) [M^{2+}]. Anal. Calcd for $C_{56}H_{52}N_4Cu$·$0.5H_2O$: C, 78.80; H, 6.26; N, 6.56. Found: C, 78.58; H, 6.28; N, 6.66.

(2,3-Diethyl-5,10,15,20-tetraphenylporphyrinato)nickel(II), Ni^{II}DETPP. Mp: >350 °C. UV/vis (CH_2Cl_2), λ_{max}, nm (log ϵ): 419 (5.41), 535 (4.25), 571 sh (3.75). ^{1}H-NMR (500 MHz, $CDCl_3$): δ 0.88 (t, ^3J = 7.5 Hz, 6H, CH_3), 2.66 (q, ^3J = 7.5 Hz, 4H, CH_2), 7.54−7.71 (m, 12H, H_{m-Ph}, H_{p-Ph}), 7.89−8.02 (m, 8H, H_{o-Ph}), 8.59 (s, 4H, $H_{pyrrole}$, 7-H, 8-H, 17-H, 18-H), 8.65 (s, 2H, $H_{pyrrole}$, 12-H, 13-H). MS, *m/z* (relative intensity, %): 726 (100) [M^+], 682 (15), 605 (27), 363 (6) [M^{2+}]. Anal. Calcd for $C_{48}H_{36}N_4Ni$: C, 79.24; H, 4.99; N, 7.70. Found: C, 79.15; H, 5.11; N, 7.66.

(2,3,12,13-Tetraethyl-5,10,15,20-tetraphenylporphyrinato)nickel-(II), Ni^{II}tTETPP. Mp: >350 °C. UV/vis (CH_2Cl_2), λ_{max}, nm (log ϵ): 423 (5.38), 544 (4.43), 581 (4.27). ^{1}H-NMR (500 MHz, $CDCl_3$): δ 0.76 (t, ^3J = 7.5 Hz, 12H, CH_3), 2.59 (q, ^3J = 7.5 Hz, 8H, CH_2), 7.59−7.70 (m, 12H, H_{m-Ph}, H_{p-Ph}), 7.98 (m, 8H, H_{o-Ph}), 8.36 (s, 4H, $H_{pyrrole}$). MS, *m/z* (relative intensity, %): 782 (100) [M^+], 738 (11), 709 (16), 391 (23) [M^{2+}]. Anal. Calcd for $C_{52}H_{44}N_4Ni$: C, 79.70; H, 5.66; N, 7.15. Found: C, 79.86; H, 5.93; N, 6.89.

(2,3,7,8-Tetraethyl-5,10,15,20-tetraphenylporphyrinato)nickel-(II), Ni^{II}cTETPP. Mp: >350 °C. UV/vis (CH_2Cl_2), λ_{max}, nm (log ϵ): 424 (5.38), 541 (4.23), 575 (3.98). ^{1}H-NMR (500 MHz, $CDCl_3$): δ 0.51, 0.72 (each t, ^3J = 7.5 Hz, 12H, CH_3), 2.31, 2.50 (each q, ^3J = 7.5 Hz, 8H, CH_2), 7.67 (m, 12H, H_{m-Ph}, H_{p-Ph}), 8.09 (m, 8H, H_{o-Ph}), 8.39, 8.44 (each d, ^3J = 5 Hz, 4H, $H_{pyrrole}$). MS, *m/z* (relative intensity, %): 782 (100) [M^+], 709 (10), 679 (11), 391 (15) [M^{2+}]. Anal. Calcd for $C_{52}H_{44}N_4Ni$: C, 79.70; H, 5.66; N, 7.15. Found: C, 79.69; H, 5.74; N, 6.84.

(2,3,7,8,12,13-Hexaethyl-5,10,15,20-tetraphenylporphyrinato)-nickel(II), Ni^{II}HETPP. Mp: >350 °C. UV/vis (CH_2Cl_2), λ_{max}, nm (log ϵ): 429 (5.36), 546 (4.43), 585 (4.31). ^{1}H-NMR (250 MHz, $CDCl_3$): δ 0.49, 0.50, 0.67 (each t, ^3J = 7.5 Hz, 18H, CH_3), 2.23, 2.28, 2.47 (each q, ^3J = 7.5 Hz, 12H, CH_2), 7.58−7.71 (m, 12H, H_{m-Ph}, H_{p-Ph}), 8.05−8.12 (m, 8H, H_{o-Ph}), 8.15 (s, 2H, $H_{pyrrole}$). MS, *m/z* (relative intensity, %): 838 (100) [M^+], 419 (18) [M^{2+}]. Anal. Calcd for $C_{56}H_{52}N_4Ni$: C, 80.07; H, 6.24; N, 6.67. Found: C, 79.89; H, 6.27; N, 6.50.

X-ray Crystallography. Suitable single crystals of the listed compounds often could be obtained by slow diffusion of a concentrated solution of the porphyrin in methylene chloride into methanol. Single crystals of H_2tTETPP and H_2HETPP were grown from CH_2Cl_2/CH_3OH containing 2% KOH. Zn^{II}DETPP(β-pic) was crystallized from CH_2Cl_2/CH_3OH containing 5% β-picoline. Zn^{II}cTETPP(pyr) and Zn^{II}HETPP(pyr) crystals were grown from CH_2Cl_2/CH_3OH containing 10% pyridine while Zn(II)tTETPP(pyr) was crystallized from $CDCl_3$/CH_3OH containing 10% pyridine. H_2DETPP crystals were obtained from $CHCl_3$/hexanes, and Cu^{II}tTETPP was crystallized from CH_2Cl_2/C_2H_5OH. The crystals were immersed in hydrocarbon oil (Paratone N), and a single crystal was selected, mounted on a glass fiber, and placed in the low-temperature N_2 stream.[20a] Intensity data were collected either using a Siemens R3m/V or Syntex $P2_1$ automatic four-circle diffractometer equipped with a graphite monochromator and locally modified low-temperature devices or using a Siemens P4 instrument equipped with a Siemens LT device and a Siemens rotating anode, operating at 50 kV and 300 mA. Cell parameters for the

(20) (a) Hope, H. *ACS Symp. Ser.* **1987**, *357*, 257; *Prog. Inorg. Chem.* **1994**, *41*, 1. (b) Parkin, S. R.; Moezzi, B.; Hope, H. *J. Appl. Crystallogr.* **1995**, *28*, 53. (c) *SHELXTL PLUS*, Version 5.03; Siemens Analytical Instruments, Inc.: Madison, WI, 1994.

structures measured with Mo Kα radiation were determined from 20−30 reflections in the range $10° \leq \theta \leq 15°$; for structures measured with Cu Kα radiation, the range $20° \leq \theta \leq 30°$ was used. Two standard reflections were measured every 198 reflections and showed only statistical variation in intensity during data collection (<2% intensity change in most cases). The intensities were corrected for Lorentz and polarization effects. With the exception of the structure of H_2DETPP, absorption corrections were applied using the program XABS2;[20b] extinction effects were mostly disregarded. The free-base porphyrin structures were solved using direct methods, while the metalloporphyrin structures were solved via Patterson syntheses followed by subsequent structure expansion using the SHELXTL PLUS program system.[20c] Refinements were carried out by full-matrix least-squares calculation based on $|F^2|$ using the same program system. Hydrogen atoms were included at calculated positions by using a riding model (C−H distance 0.96 Å, N−H distance 0.9 Å). Normally, no hydrogen atoms were included for solvate molecules. All calculations were carried out on a Silicon Graphics Indy workstation. Unless otherwise stated, all non-hydrogen atoms were refined with anisotropic thermal parameters.

In the structures of H_2tTETPP, Ni^{II}DETPP, Ni^{II}tTETPP, and Zn(II)HETPP, the phenyl rings were refined with isotropic thermal parameters as rigid groups (hexagon with C−C distances of 1.39 Å). H_2tTETPP crystallized with two disordered methylene chloride molecules of solvation. The chlorine atoms were refined as disordered over two and three split positions. A similar situation was encountered in the structure of H_2HETPP. One solvate methylene chloride was refined with the chlorine atoms disordered over two (Cl1S) and three (Cl2S) split positions. The other CH_2Cl_2 molecule was situated on an inversion center and was refined with 30% occupancy. The crystals of Ni^{II}tTETPP were twinned and refined using the TWIN routine of the XL program. Due to the twinning, some of phenyl carbon atoms showed relatively high thermal parameters. Attempts to utilize disorder models for the phenyl rings failed and resulted in unreasonably distorted phenyl rings. In the structure of Ni^{II}HETPP, only the nickel and side chain ethyl and phenyl carbon atoms were refined with anisotropic thermal parameters. Cu^{II}cTETPP was refined with isotropic thermal parameters for the phenyl carbon atoms. The structure of Zn^{II}tTETPP-(pyr) contains a disordered axial pyridine. The axial ligand was refined as disordered over two split positions with occupancies of 0.6 and 0.4, each. To account for residual electron density close to the major pyridine fraction, a water molecule was included in the refinement which refined with an occupancy similar to that of the minor pyridine form (0.4). Only the nondisordered positions were refined with anisotropic thermal parameters. For refinement of Zn^{II}HETPP, each group of C_a, C_b, and C_m atoms was refined with a common isotropic temperature factor. Only the zinc, nitrogen, and side chain ethyl carbon atoms were refined with anisotropic thermal parameters. For Zn^{II}-cTETPP, a second crystalline modification was found which crystallized in the triclinic system with unit cell parameters of $a = 10.414(8)$ Å, $b = 13.237(22)$ Å, $c = 16.240(25)$ Å, $\alpha = 65.95(10)°$, $\beta = 80.38(10)°$, $\gamma = 81.06(10)$, $V = 1991(4)$ Å^3, and $Z = 2$. Due to the high esd's observed for the unit cell parameters, no data collection was performed.

Further details of the crystal data and structure solutions and refinements are listed in Table 1 and have been deposited with the CCDC.

Results and Discussion

For synthesis of the desired porphyrins, the method of mixed condensation was used. An equimolar solution of pyrrole, diethylpyrrole, and benzaldehyde was treated with $BF_3 \cdot OEt_2$ as catalyst for 2 h. Subsequent oxidation of the porphyrinogens formed in situ yielded a mixture of all six possible compounds. The mixture was easily separated by alumina column chromatography into three fractions, each containing two products. While the fractions containing H_2TPP/H_2DETPP or H_2tTETPP/H_2cTETPP could easily be separated by a second chromatographic step using silica gel or alumina, respectively, separation of the fraction containing H_2HETPP/H_2OETPP proved to be more difficult. Although separation of these compounds is possible via repeated column chromatography on alumina, this process is quite laborious. More convenient and less time-consuming was conversion of the crude mixture containing H_2-HETPP and H_2OETPP to the respective $Fe^{III}Cl$ or Ni^{II} complexes. The iron(III) complexes could be purified easily by conventional column chromatography on alumina, while preparative HPLC chromatography using a silica gel column was required for the Ni(II) complexes.

Table 2. Soret and Long-Wavelength Q-Band Absorption Maxima of the Porphyrins Studied in Methylene Chloride

	M									
	H_2[a] free base		H_4^{2+}[b] dication		Ni(II)		Zn(II)		Cu(II)	
porphyrin										
OEP	397	618	401	591	391	551	400	567	398	560
TPP	417	647	436	653	415	525	419	578	n.d.	n.d.
DETPP	420[a]	645[a]	445	663	419	571	420	582 sh	417	543
tTETPP	426[a]	649[a]	451	668	423	581	424	586 sh	422	552
cTETPP	433[a]	672[a]	455	675	424	575	431	611	424	562
HETPP	444[a]	685[a]	462	683	429	585	443	625	429	566
OETPP	456[a]	706[a]	468	687	432	585	455	643	430	598

[a] Spectra taken in methylene chloride containing % NEt_3. [b] Spectra taken in methylene chloride containing % TFA.

A simple test for the relative conformation of the free-base porphyrins in solution can be performed by inspection of their electronic absorption spectra.[5c] All studies on porphyrin nonplanarity have shown that increasing macrocycle distortion is accompanied by an increasing bathochromic shift of the absorption bands. These red shifts are due to the destabilization of the π-system, which mainly results in an increase of the HOMO level and smaller perturbations of the LUMO.[1c] Table 2 lists the main absorption maxima of the compounds studied and clearly shows that the absorption bands are successively red-shifted and broadened with increasing number of β-ethyl substituents. Since the number and positions of the diethylpyrrole units should correspond to the degree of conformational distortion the following order of nonplanarity is obtained: H_2-OETPP > H_2HETPP > H_2cTETPP > H_2tTETPP > H_2DETPP > H_2TPP.

In addition, UV/vis spectroscopy provides evidence for the importance of the individual substituent pattern. Both regioisomers of TETPP bear the same number and type of substituents. In general, two types of steric hindrance are present in these compounds. The meso-phenyl substituents are flanked either by two β-hydrogen atoms (H−Ph−H), by a β-ethyl and a β-hydrogen substituent (Et−Ph−H), or by two β-ethyl substituents (Et−Ph−Et). The steric strain imposed on the macrocycle by these groups follow the order Et−Ph−Et > Et−Ph−H > H−Ph−H. Indeed, H_2cTETPP, which contains one Et−Ph−Et and two Et−Ph−H units, shows a significantly bathochromically shifted absorption spectrum compared to H_2-tTETPP, which only has Et−Ph−H units. Similar results were obtained for the corresponding porphyrin dications. Increasing nonplanarity in solution is also evident from ^{1}H-NMR spectra. The N−H protons show increasing deshielding in the order H_2-DETPP < H_2tTETPP < H_2cTETPP < H_2HETPP ($\delta = -3.04/-2.45$, -2.60, -2.38, and -2.23 ppm, respectively).

Besides a stepwise increase in nonplanarity upon going from TPP to OETPP, we expected to see asymmetric distortion modes for the intervening porphyrins. Thus, in order to determine the exact macrocycle conformations, single-crystal X-ray structure determinations were performed for all compounds. In contrast to our experience with some other highly substituted porphyrins, the present compounds could be crystallized quite easily.

Figure 1 shows side views of the four new free-base porphyrins H_2DETPP, H_2tTETPP, H_2cTETPP, and H_2HETPP

Table 3. Macrocycle Conformations of the Porphyrins Studied[a]

		C_b displacement, Å										pyrrole tilt, deg				
			quadrant				C_m displacement, Å						quadrant			
compd	Δ24,[b] Å	av	N21	N22	N23	N24	av	C5	C10	C15	C20	av	N21	N22	N23	N24
H_2OEP[21]	0.02	0.08	0.06	0.11	*d*	*d*	0.04	0.03	0.05	*d*	*d*	1.7	2.2	1.1	*d*	*d*
H_2TPP, tricl[22a]	0.05	0.06[c]	0.03	0.09	*d*	*d*	0.04[c]	0.05	0.03	*d*	*d*	4.0	6.6	1.4	*d*	*d*
H_2TPP, tetrag[22b]	0.19	0.14	0.14	*d*	*d*	*d*	0.38	0.38	*d*	*d*	*d*	11.9	11.9	*d*	*d*	*d*
H_2DETPP	0.10	0.19	0.29	0.04	0.15	0.29	0.05	0.06	0.03	0.05	0.06	4.3	6.8	0.5	3.1	6.7
H_2tTETPP	0.29	0.61	0.64	0.59	0.62	0.57	0.04	0.01	0.05	0.05	0.06	15.0	16.3	14.1	15.9	13.7
H_2cTETPP	0.38	0.76	0.93	1.24	0.57	0.31	0.12	0.18	0.03	0.04	0.20	20.4	25.1	33.7	14.8	7.8
H_2HETPP	0.46	0.95	0.79	1.17	1.08	0.74	0.06	0.05	0.01	0.08	0.10	24.0	20.3	29.0	28.6	17.9
H_2OETPP[10a]	0.54	1.17	1.03	1.27	1.26	1.10	0.03	0.07	0.05	0	0.01	31.2	26.7	34.8	33.5	29.7
Ni^{II}OEP, tricl A[23b]	0.02	0.06	0.06	0.06	*d*	*d*	0.03	0.04	0.01	*d*	*d*	1.7	1.6	1.8	*d*	*d*
Ni^{II}OEP, tetrag[23a]	0.26	0.27	0.27	*d*	*d*	*d*	0.51	0.51	*d*	*d*	*d*	16.4	16.4	*d*	*d*	*d*
Ni^{II}DETPP	0.45	0.82	0.88	0.81	0.79	0.81	0.28	0.34	0.30	0.24	0.23	21.0	23.5	20.9	19.2	20.3
Ni^{II}tTETPP[e]	0.39	0.32	0.33	0.30	*d*	*d*	0.79	0.78	0.79	*d*	*d*	25.7	26.6	24.7	*d*	*d*
	0.46	0.61	0.70	0.51	*d*	*d*	0.68	0.69	0.68	*d*	*d*	26.1	27.5	24.6	*d*	*d*
Ni^{II}cTETPP	0.49	0.89	1.08	1.00	0.78	0.71	0.20	0.23	0.14	0.21	0.20	20.8	26.8	23.3	17.0	16.2
Ni^{II}HETPP	0.53	1.00	1.11	1.04	1.03	0.82	0.16	0.24	0.14	0.13	0.13	23.4	26.5	24.8	23.9	18.2
Ni^{II}OETPP[9]	0.62	1.25	1.19	1.27	1.26	1.27	0.03	0	0.03	0.06	0.03	29.4	27.7	30.2	29.3	30.5
Cu^{II}TPP[24]	0.21	0.16	0.16	*d*	*d*	*d*	0.42	0.42	*d*	*d*	*d*	13.4	13.4	*d*	*d*	*d*
Cu^{II}OEP[25]	0.02	0.05	0.02	0.08	*d*	*d*	0.01	0.01	0.01	*d*	*d*	1.5	0.9	2.0	*d*	*d*
Cu^{II}DETP[e]	0.32	0.58	0.73	0.45	0.62	0.52	0.16	0.22	0.03	0.19	0.18	13.9	18.3	10.1	14.1	12.9
	0.26	0.52	0.55	0.59	0.36	0.58	0.07	0.04	0.12	0.06	0.07	12.2	13.2	14.0	7.7	13.7
Cu^{II}tTETPP	0.40	0.73	0.86	0.63	0.69	0.73	0.23	0.23	0.29	0.20	0.19	18.1	21.2	15.5	18.0	17.8
Cu^{II}cTETPP	0.44	0.83	1.09	0.97	0.67	0.58	0.17	0.21	0.15	0.20	0.12	19.8	27.2	23.5	15.1	13.4
Cu^{II}HETPP	0.49	0.95	1.10	1.01	0.99	0.71	0.13	0.21	0.11	0.13	0.05	23.0	27.0	24.8	24.0	16.2
Cu^{II}OETPP[8]	0.55	1.13	1.12	1.07	1.13	1.18	0.04	0.02	0.02	0.04	0.09	27.4	27.3	25.6	27.6	29.1
Zn^{II}TPP(H_2O)[26a]	0.01	0	0	*d*	*d*	*d*	0	0	*d*	*d*	*d*	0	0	*d*	*d*	*d*
Zn^{II}TPP, tricl[26b]	0.05	0.21	0.34	0.08	*d*	*d*	0.15	0.17	0.12	*d*	*d*	6.5	9.1	3.1	*d*	*d*
Zn^{II}OEP(pyr)[27]	0.06	0.16	0.27	0.17	0	0.21	0.08	0.07	0.05	0.06	0.12	4.1	7.4	4.0	0.5	4.7
Zn^{II}DETPP(MeOH)	0.06	0.12	0.24	0.11	0.09	0.03	0.02	0.01	0.01	0	0.05	3.1	6.4	3.0	2.3	0.7
Zn^{II}DETPP(β-pic)	0.18	0.25	0.31	0.41	0.09	0.17	0.17	0.15	0.14	0.05	0.34	9.3	11.5	11.1	3.0	11.4
Zn^{II}tTETPP(pyr)	0.28	0.54	0.35	0.61	0.68	0.50	0.20	0.33	0.14	0.19	0.15	15.0	10.5	16.9	18.4	14.0
Zn^{II}cTETPP(pyr)	0.33	0.63	0.79	0.92	0.21	0.60	0.18	0.23	0.08	0.27	0.15	16.9	20.8	24.1	7.2	15.6
Zn^{II}HETPP	0.45	0.84	1.08	1.00	0.98	0.28	0.12	0.20	0.11	0.16	0	22.5	27.1	25.4	24.5	13.0
Zn^{II}HETPP(pyr)	0.43	0.89	0.86	1.10	0.85	0.74	0.06	0.05	0.04	0.02	0.11	22.4	21.8	28.4	21.4	17.9
Zn^{II}OETPP(MeOH)[7]	0.50	1.09	1.02	1.09	1.21	1.03	0.04	0.02	0.08	0	0.06	28.4	26.2	28.7	31.7	26.9

[a] Numbers are given relative to the least-squares plane for the four nitrogen atoms. Numbers listed for individual quadrants give the average values of geometrically equivalent positions in each quadrant. [b] Average deviation of the 24 macrocycle atoms from their least-squares plane. [c] Data relative to 24 macrocycle atom plane. [d] Generated by symmetry operation. [e] Two crystallographically independent molecules.

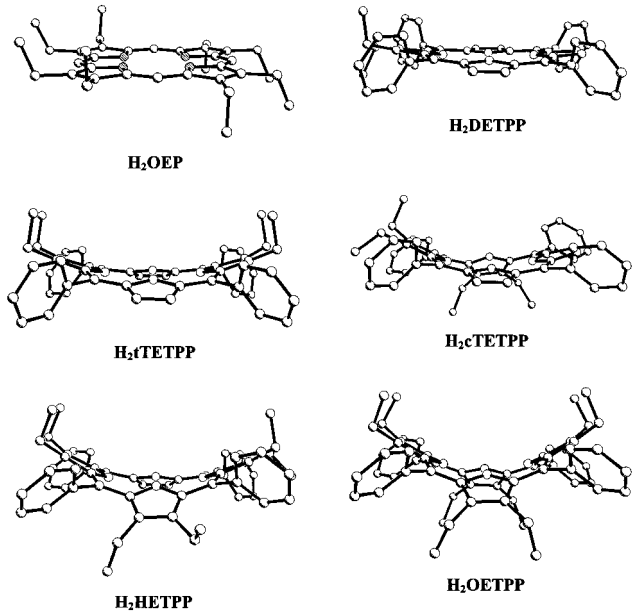

Figure 1. Side views of the molecular structures of H_2OEP, H_2DETPP, H_2tTETPP, H_2cTETPP, H_2HETPP, and H_2OETPP.

and those of H_2OEP[21] and H_2OETPP.[10a] Even a rudimentary visual inspection shows that the porphyrins become progressively more nonplanar in the order H_2OEP < H_2DETPP < H_2tTETPP < H_2cTETPP < H_2HETPP < H_2OETPP. A good measure for the overall degree of nonplanarity in a porphyrin is the average deviation of the 24 macrocycle atoms from their least-squares plane. As indicated in Table 3, these Δ24 values increase in the same order with values of 0.02, 0.10, 0.29, 0.38, 0.46, and 0.54 Å, respectively. This ordering of the porphyrins in the solid state gives the same result as was described above for the situation in solution on the basis of the electronic absorption spectra. For TPP, the starting compound in the series presented here, two different crystalline modifications are known.[22] While triclinic TPP (Δ24 = 0.05 Å) is more or less planar,[22a] tetragonal TPP has a ruffled conformation with Δ24 = 0.19 Å.[22b] All free-base ethyl-TPP compounds presented here exhibit saddle-distorted macrocycles, i.e. out-of-plane rotation of the pyrrole rings with large deviations observed for the C_b-positions while the C_m positions remain in the plane of the molecule. Thus, triclinic H_2TPP was chosen as reference compound for the ethyl-substituted TPP's.

A display of the skeletal deviations shows not only that the macrocycles become progressively more distorted with increasing number of β-ethyl substituents but also that the distortion modes are asymmetric in relation to the substituent pattern (Figure 2). In general, the largest deviations are observed for C_b positions in quadrants of the molecule bearing β-ethyl groups. Here two different situations have to be considered. Either

(21) Lauher, J. W.; Ibers, J. A. *J. Am. Chem. Soc.* **1973**, *95*, 5148.

(22) (a) Silvers, S. J.; Tulinsky, A. *J. Am. Chem. Soc.* **1967**, *89*, 3331. (b) Hamor, M. J.; Hamor, T. A.; Hoard, J. L. *J. Am. Chem. Soc.* **1964**, *86*, 1938.

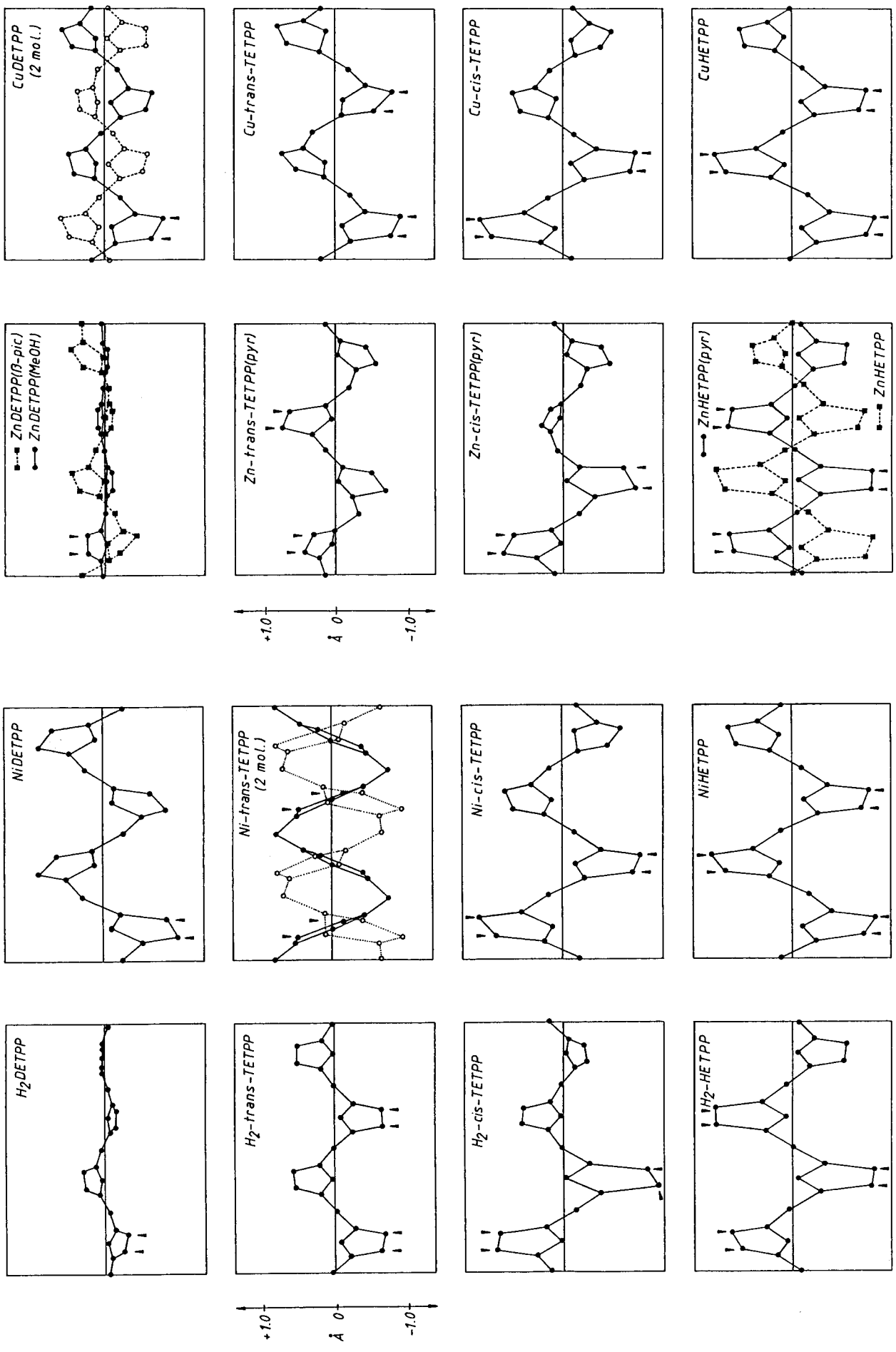

Figure 2. Linear display of the skeletal deviations of the 24 macrocycle atoms from the least-squares plane of the four nitrogen atoms. Wedges indicate β-ethyl-substituted positions.

Table 4. Core Conformations of the Porphyrins Studied (Data Given in Å)

compd	M−N[a] av	M−N21	M−N22	M−N23	M−N24	M−L_{ax}	ΔM[b]	core size av
H_2OEP, tricl[21]	2.062	2.026	2.098	*c*	*c*			2.062
H_2TPP, tricl[22a]	2.06	2.03	2.10	*c*	*c*			2.06
H_2TPP, tetrag[22b]	2.054	2.054	*c*	*c*	*c*			2.054
H_2DETPP	2.064	2.166	1.974	2.135	1.980			2.064
H_2tTETPP	2.057	2.139	1.976	2.139	1.974			2.057
H_2cTETPP	2.070	2.114	2.058	2.094	2.015			2.070
H_2HETPP	2.049	2.133	1.974	2.142	1.948			2.049
H_2OETPP[10a]	2.051	2.042	2.057	2.034	2.072			2.051
Ni^{II}OEP, tricl A[23b]	1.958(2)	1.959(2)	1.957(2)	*c*	*c*		0	1.958
Ni^{II}OEP, tetrag[23a]	1.929(3)	1.929(3)	*c*	*c*	*c*		0	1.929
Ni^{II}DETPP	1.923(6)	1.942(6)	1.916(6)	1.921(6)	1.911(6)		0	1.922
Ni^{II}tTETPP[d]	1.893(6)	1.914(6)	1.871(6)	*c*	*c*		0.03	1.896
	1.893(6)	1.899(6)	1.887(6)	*c*	*c*		0	1.894
Ni^{II}cTETPP	1.923(4)	1.930(4)	1.932(3)	1.907(4)	1.921(3)		0.01	1.923
Ni^{II}HETPP	1.921(3)	1.938(3)	1.910(3)	1.931(3)	1.905(3)		0.01	1.921
Ni^{II}OETPP[9]	1.906(2)	1.911(2)	1.901(2)	1.905(2)	1.906(2)		0.01	1.906
Cu^{II}TPP[24]	1.981(7)	1.981(7)	*c*	*c*	*c*		0	1.981
Cu^{II}OEP[25]	1.998(3)	1.996(3)	1.999(3)	*c*	*c*		0	1.998
Cu^{II}DETPP[d]	1.990(3)	2.027(3)	1.959(3)	2.012(3)	1.960(4)		0.05	1.989
	1.999(3)	2.027(3)	1.977(3)	2.014(3)	1.976(3)		0.02	1.999
Cu^{II}tTETPP	1.984(4)	2.021(4)	1.945(3)	2.017(4)	1.953(4)		0.02	1.984
Cu^{II}cTETPP	1.975(5)	1.989(5)	1.979(5)	1.962(5)	1.970(5)		0.02	1.975
Cu^{II}HETPP	1.980(5)	2.009(5)	1.960(4)	2.001(5)	1.950(5)		0.02	1.980
Cu^{II}OETPP[8]	1.977(5)	1.959(5)	1.991(5)	1.970(5)	1.990(5)		0	1.978
Zn^{II}TPP(H_2O)[26a]	2.050(3)	2.050(3)	*c*	*c*	*c*	2.228(12)	0.17	2.043
Zn^{II}TPP, tricl[26b]	2.037(3)	2.029(2)	2.045(2)	*c*	*c*		0	2.037
Zn^{II}OEP(pyr)[27]	2.067(6)	2.068(3)	2.062(3)	2.061(3)	2.075(3)	2.200(3)	0.31	2.043
Zn^{II}DETPP(MeOH)	2.062(5)	2.091(5)	2.030(5)	2.101(5)	2.026(5)	2.217(5)	0.21	2.052
Zn^{II}DETPP(β-pic)	2.068(4)	2.099(4)	2.043(4)	2.086(4)	2.045(4)	2.165(4)	0.32	2.043
Zn^{II}tTETPP(pyr)	2.071(3)	2.094(3)	2.048(4)	2.108(3)	2.034(4)	2.182(6)	0.31	2.048
Zn^{II}cTETPP(pyr)	2.070(3)	2.075(3)	2.071(3)	2.062(3)	2.072(3)	2.177(3)	0.32	2.045
Zn^{II}HETPP	2.028(4)	2.068(4)	1.995(5)	2.057(4)	1.991(4)		0.07	2.026
Zn^{II}HETPP(pyr)	2.069(3)	2.091(3)	2.052(3)	2.086(3)	2.046(3)	2.131(3)	0.35	2.039
Zn^{II}OETPP(MeOH)[7]	2.063(5)	2.069(5)	2.056(5)	2.072(5)	2.051(5)	2.226(5)	0.22	2.048

[a] For the free-base porphyrins, M refers to the geometrical center of the N_4 least-squares plane. [b] Displacement of the metal from N_4 plane. [c] Generated by symmetry operation. [d] Two crystallographically independent molecules.

diethylpyrrole ring can be situated next to a meso-phenyl which is flanked by a β-H and a β-ethyl group (Et−Ph−H) or alternatively it can be part of a Et−Ph−Et group. The latter type of pyrrole ring is encountered in cTETPP and HETPP (and OETPP), and as expected, individual pyrrole displacements in these compounds are even larger.

H_2tTETPP exhibited an almost symmetric distortion mode with only minor differences between individual quadrants—an indication of the extent to which steric strain can be redistributed. The fact that the distortion of β-hydrogen-substituted pyrrole units exceeded those of the unsubstituted positions in H_2cTETPP has to be due to the different steric building blocks. The latter has a H−Ph−H unit in the "southern" region, while H_2tTETPP contains only Et−Ph−H blocks. Similar results are obtained if the angles formed between individual pyrrole rings and the N_4 plane are inspected (Table 3).

The local effect of macrocycle distortion is best evidenced by the fact that individual displacements can reach those observed in dodecasubstituted porphyrins. For example ring II in H_2cTETPP shows C_b displacements (1.24 Å) and pyrrole tilt angles (33.7°) which are very similar to the largest ones described for H_2OETPP (1.27 Å and 34.8°).[10a] However, this statement has to be viewed with some caution. Redistribution of steric strain does occur and the macrocycle for a given macrocycle is relatively flexible, leaving room for packing and aggregation forces.[14] This is clearly evidenced by significant distortions for ring III in H_2DETPP or the inequivalence of the deviations observed for the pairs of pyrrole rings bearing either β-ethyl or β-hydrogen substituents in H_2cTETPP. Nevertheless, the differences between chemically equivalent groups become smaller with increasing overall degree of macrocycle distortion.

The possibility remained that part of the steric strain is relieved by in-plane distortion of the macrocycle. Such effects have been described for 2,3,5,7,8,12,13,15,17,18-decasubstituted porphyrins and are characterized by in-plane elongation of the porphyrin core, leading to inequivalency of different N−N vectors.[28] No evidence for this was found. In addition, for all compounds described here, packing analyses were performed. Generally, with increasing degree of nonplanarity, the packing types deviated more and more from the layer-type structures observed for planar porphyrins and came closer to the interlocking fit often observed for highly nonplanar porphyrins.[5−14] However, in distinction to the symmetric, dodecasubstituted porphyrins in several cases, weak $\pi-\pi$ aggregates were observed for the asymmetric porphyrins described here. These were characterized by interplanar separations between neighboring molecules in the range 3.5−4 Å and lateral shifts of the porphyrin centers in the range 3.5−4.6 Å. According to the classification given by Scheidt and Lee,[14] these interactions fall into the intermediate/weak category. Since this effect did not correlate with any of the conformational parameters and otherwise the molecules were well separated, the influence of crystal packing forces was deemed to be low and the observed out-of-plane displacements have to be mainly due to the steric strain imposed by the peripheral substituents.

Structural data on the core conformation (Table 4) and the bond lengths and angles (Table 5) show that structural differences between pyrrole rings containing N−H hydrogens and those without are retained in the nonplanar porphyrins. This is evidenced by longer N−Ct vector lengths and wider C_a−N−C_a angles for N−H pyrrole rings (Ct is defined as the geometrical center of the N_4 unit). Bond lengths and bond

Table 5. Selected Bond Lengths (Å) and Angles (deg) for the Free-Base Porphyrins Studied

	quadrant	H_2OEP[21]	H_2TPP, tricl[22a]	H_2TPP, tetr[22b]	H_2DETPP	H_2tTETPP	H_2cTETPP	H_2HETPP	H_2OETPP[a,10a]
$N-C_a$	N21	1.364(2)	1.376	1.350(7)	1.377(5)	1.383(9)	1.381(5)	1.368(6)	1.368
	N22	1.367(2)	1.365	*b*	1.376(5)	1.366(9)	1.365(5)	1.363(6)	
	N23	*b*	*b*	*b*	1.373(5)	1.377(9)	1.379(5)	1.369(6)	
	N24	*b*	*b*	*b*	1.370(5)	1.367(9)	1.366(5)	1.374(7)	
C_a-C_b	N21	1.438(2)	1.428	1.438(8)	1.447(5)	1.430(10)	1.444(5)	1.450(7)	1.451
	N22	1.463(2)	1.455	*b*	1.456(5)	1.459(10)	1.465(6)	1.460(7)	
	N23	*b*	*b*	*b*	1.430(5)	1.441(10)	1.427(6)	1.446(7)	
	N24	*b*	*b*	*b*	1.458(5)	1.452(10)	1.457(5)	1.451(7)	
C_b-C_b	N21	1.373(2)	1.355	1.362(9)	1.380(5)	1.369(10)	1.379(6)	1.368(7)	1.377
	N22	1.363(2)	1.347	*b*	1.345(6)	1.336(10)	1.374(6)	1.361(8)	
	N23	*b*	*b*	*b*	1.357(6)	1.370(10)	1.354(5)	1.375(7)	
	N24	*b*	*b*	*b*	1.342(6)	1.337(11)	1.342(5)	1.337(8)	
C_a-C_m	N21	1.390(2)	1.400	1.403(7)	1.402(5)	1.400(10)	1.414(6)	1.396(7)	1.407
	N22	1.394(2)	1.400	*b*	1.410(5)	1.401(10)	1.411(5)	1.424(7)	
	N23	*b*	*b*	*b*	1.397(5)	1.401(10)	1.405(5)	1.400(7)	
	N24	*b*	*b*	*b*	1.409(5)	1.404(10)	1.407(5)	1.399(7)	
C_a-N-C_a	N21	109.6(1)	109.2	108.9(4)	110.8(3)	109.6(6)	110.7(3)	111.9(4)	106.1
	N22	105.7(1)	106.2	*b*	104.8(3)	106.6(6)	106.3(3)	105.1(4)	111.0
	N23	*b*	*b*	*b*	110.8(3)	110.4(6)	110.4(3)	112.4(4)	
	N24	*b*	*b*	*b*	105.0(3)	106.0(6)	105.7(3)	105.3(4)	
$N-C_a-C_b$	N21	107.8(1)	107.3	107.5(4)	106.8(3)	106.9(6)	106.6(3)	105.9(4)	108.7
	N22	110.9(1)	110.3	*b*	110.9(3)	109.7(6)	110.7(3)	111.2(4)	
	N23	*b*	*b*	*b*	106.3(3)	106.6(6)	106.1(3)	105.5(4)	
	N24	*b*	*b*	*b*	111.0(3)	110.6(6)	110.5(3)	110.3(5)	
$C_a-C_b-C_b$	N21	107.4(1)	108.1	106.9(5)	107.8(3)	108.2(6)	108.0(3)	108.1(5)	106.9
	N22	106.3(1)	106.8	*b*	106.7(3)	107.0(6)	106.1(4)	106.0(5)	
	N23	*b*	*b*	*b*	108.4(4)	108.1(6)	108.6(4)	108.2(5)	
	N24	*b*	*b*	*b*	106.6(4)	107.0(7)	106.7(4)	107.0(5)	
$N-C_a-C_m$	N21	125.0(1)	126.0	126.0(5)	124.1(3)	122.6(6)	123.6(3)	123.1(5)	122.4
	N22	125.1(1)	126.3	*b*	126.9(4)	127.4(6)	123.0(3)	122.3(5)	
	N23	*b*	*b*	*b*	125.8(3)	123.2(6)	125.6(3)	123.1(5)	
	N24	*b*	*b*	*b*	127.0(4)	126.8(7)	126.1(4)	125.7(5)	
$C_a-C_m-C_a$	N21	127.4(1)	125.6	125.2(5)	126.4(3)	125.8(7)	124.6(4)	124.3(5)	123.8
	N22	127.7(1)	125.6	*b*	124.6(4)	124.6(6)	124.1(3)	124.9(5)	
	N23	*b*	*b*	*b*	125.6(3)	126.0(6)	124.3(4)	124.1(5)	
	N24	*b*	*b*	*b*	126.0(3)	125.9(7)	124.8(3)	126.2(5)	
$C_m-C_a-C_b$	N21	127.3(1)	126.2	125.1(5)	129.2(3)	130.5(7)	129.7(4)	130.8(5)	128.8
	N22	124.0(1)	123.5	*b*	122.2(4)	122.9(6)	126.1(4)	126.2(5)	
	N23	*b*	*b*	*b*	127.9(4)	130.2(6)	128.1(4)	131.4(5)	
	N24	*b*	*b*	*b*	121.9(4)	123.2(7)	123.2(3)	123.9(5)	

[a] Average data for geometrically equivalent positions. [b] Generated by symmetry operation.

angles for individual quadrants of the porphyrins also give evidence for the influence of increasing macrocycle distortion. C_a-C_b, C_b-C_b, and C_a-C_m bonds become more elongated and $N-C_a-C_m$ and $C_a-C_m-C_a$ angles become smaller, while $C_m-C_a-C_b$ angles are larger in nonplanar macrocycles. Although these results agree well with those for symmetric nonplanar porphyrins,[5−13] the novel, less symmetric porphyrins presented here give evidence for the local influence of the different substituent patterns. Areas of the porphyrin macrocycle with steric hindrance yield geometrical data which resemble those of the highly nonplanar H_2OETPP, while parts of the molecules without steric strain exhibit bond lengths and angles closer to those of their planar counterparts. In some instances, the relative trends of individual geometrical parameters for sterically hindered macrocycle parts even exceed those found for H_2-OETPP when compared to H_2TPP or H_2OEP. For example, the C_b-C_b bond length in pyrrole N21 of H_2DETPP (1.380 Å) is considerably longer than the average for triclinic H_2TPP (1.351 Å)[22a] or H_2OEP (1.368 Å)[21] and slightly longer than the average found in H_2OETPP (1.377 Å), despite the fact that the latter is considerably more distorted than H_2DETPP. This presents further evidence for the local influence of peripheral steric strain.

In order to study the influence of different metals on the conformation, metal complexes with M = Ni(II), Zn(II), and Cu(II) were prepared via metalation with metal acetates or metal bromides. Inspection of the absorption spectra (Table 2) showed an ordering of the metal complexes similar to that observed for the free bases and dications on the basis of the bathochromic shift of the absorption bands: M^{II}OETPP > M^{II}HETPP > M^{II}cTETPP > M^{II}tTETPP > M^{II}DETPP > M^{II}TPP. The only exception to this ordering was observed for the Ni(II) complexes of cTETPP and tTETPP. Here the ordering found for the other series was reversed and Ni^{II}tTETPP showed a more red-shifted Q absorption band (λ_{max} = 581 nm) than Ni^{II}cTETPP (λ_{max} = 575 nm).

The crystal structures of the nickel(II) complexes (Figure 2) show that three of the four new porphyrins (Ni^{II}DETPP, Ni^{II}cTETPP, and Ni^{II}HETPP) exhibit saddle-distorted macrocycles. This is in agreement with the results for dodecasubstituted porphyrins with peripheral steric strain induced by β-alkyl and meso-aryl groups, which all have been described as saddle conformations.[9] Compared to the free-base porphyrins and to Ni^{II}OETPP, these porphyrins showed a significant degree of ruffling, as indicated by average C_m displacements on the order of 0.2 Å (Table 3) and by the tilt of the pyrrole rings in their plane (Figure 2). While saddle conformations are characterized by large displacements of the C_b-position, ruffled conformations are characterized by significant C_m displacements and an in-plane rotation of the pyrrole rings.[14]

Ruffled conformations are often found for metalloporphyrins with small metal ions, which tend to distort the macrocycle in order to minimize their M−N bonds. The best known example

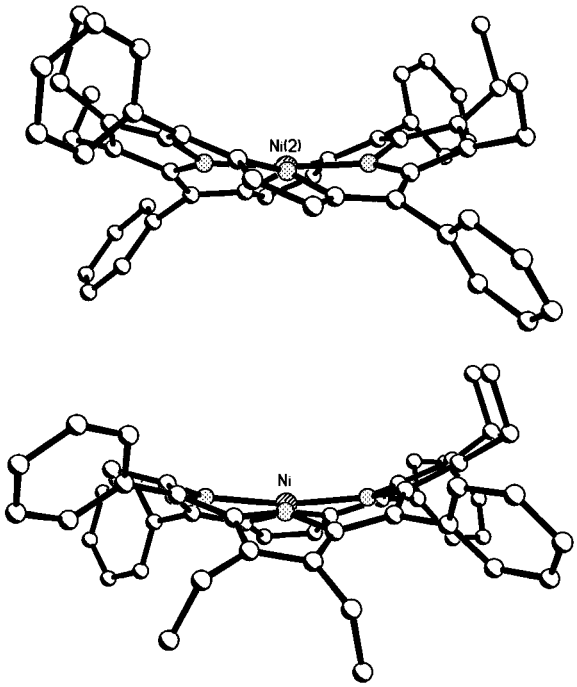

Figure 3. Side views of the molecular structures of one of the two independent molecules in the structures of Ni^{II}tTETPP (top) and Ni^{II}cTETPP (bottom). Hydrogen atoms and disordered positions have been omitted for clarity. Both views have the same orientation with the N_4 plane orthogonal to the plane of the paper and the macrocycle viewed along a N−Ni−N axis.

of a metalloporphyrin with different conformations is Ni^{II}OEP,[23] which has been found in both planar and severely ruffled modifications (C_m displacements of 0.51 Å).[23a] Similarly, (2:3,7:8,12:13,17:18-tetracyclopenteno-5,10,15,20-tetrakis(3,4,5-trimethoxyphenyl)porphyrinato)nickel(II) [$Ni^{II}TC_5$TPOMeP], a porphyrin for which no steric strain was expected due to the small size of the five membered cyclopenteno rings and for which molecular mechanics calculations[5c] and EXAFS investigations[9] had predicted a planar conformation, was found to exhibit a ruffled conformation in the solid state due to crystal packing forces (C_m displacements 0.60 Å).[5c]

As noted above, an exception to the order of nonplanarity established for the free-base porphyrins was found for Ni^{II}cTETPP and Ni^{II}tTETPP. As shown in Figures 2 and 3, this is due to the fact that Ni^{II}tTETPP, in contrast to all other structures described in this paper, has a ruffled conformation. The compound crystallized with two independent molecules which are mainly differentiated by the degree of in-plane rotation of the pyrrole rings. The degree of ruffling is severe; average C_m displacements for both molecules are 0.68 and 0.79 Å which is significantly more than the values described in the preceding paragraph for $Ni^{II}TC_5$TPOMeP and Ni^{II}OEP.

Overall, the nickel(II) porphyrins gave results similar to those obtained for the respective free-base porphyrins. Thus, areas of the porphyrins with steric strain exhibited larger distortions from planarity with associated changes in their bond lengths and angles (Table 6). Larger differences were found if less highly substituted nickel(II) and free-base porphyrins are compared, e.g. DETPP. Here, the differences between regions with peripheral steric strain and those without are much less pronounced in the nickel(II) compound. Upon going to more highly substituted porphyrins like cTETPP or HETPP, the relative magnitudes of the differences between peripherally sterically strained regions and those with β-hydrogen substituents are similar in the free-base and nickel(II) porphyrins. A possible explanation for this effect, which is also found for the respective Cu(II) porphyrins (see below), might be that the less highly substituted porphyrins can pack more closely in the crystal and thus packing forces can exert more influence in these compounds than in the more highly substituted porphyrins.

For a given distortion mode, e.g. saddle or ruffle, increasing macrocycle distortion leads to shorter average M−N bond lengths. Crystal structure analysis of the DETPP, tTETPP, cTETPP, and HETPP metalloporphyrins presented here shows that this is achieved in asymmetrically substituted porphyrins mainly via shortening of the M−N bond lengths involving the less distorted regions. M−N bond lengths to pyrrole rings deviating strongly from the mean plane are generally longer than those involving more planar quadrants of the macrocycle. A typical example is Ni^{II}cTETPP, which shows average Ni−N bond lengths of 1.931 Å for the ethyl-substituted pyrroles (average tilt angle against the N_4 plane 25.1°) and 1.914 Å for the hydrogen-substituted pyrroles (average tilt angle 16.6°). Similar conclusions are possible for the ruffled Ni^{II}tTETPP, which has an average Ni−N bond length of 1.893 Å (ΔC_m = 0.68, 0.79 Å). This is shorter than the 1.929 Å found for tetragonal Ni^{II}OEP (ΔC_m = 0.51 Å)[23a] or the 1.917 Å described for $Ni^{II}TC_5$TPOMeP (ΔC_m = 0.60 Å).[5c] Interestingly, it is still shorter than the 1.909(5) Å described for a ruffled (dodecaphenylporphyrinato)nickel(II) [Ni^{II}DPP], which exhibited C_m displacements of 0.86 Å.[11c] Ruffling can also be induced by introduction of sterically demanding meso-alkyl groups.[11b,15] Such compounds show structural data similar to those for Ni^{II}tTETPP. For example, (2:3,7:8,12:13,17:18-tetracyclopenteno-5,10,15,20-tetra-*n*-pentylporphyrinato)nickel(II) has an average Ni−N bond length of 1.911 Å and C_m displacements of 0.83 Å,[11b] while (5,10,15,20-tetraisopropylporphyrinato)-nickel(II) has an average Ni−N bond length of 1.896 Å and C_m displacements of 0.74 Å.[15a] The shortest experimentally determined Ni−N bond length of 1.88 Å has been described on the basis of EXAFS data in toluene for Ni^{II}DPP.[9]

As evidenced by structural data for H_2tTETPP, steric strain is present in the tTETPP system. Thus, the observation of a ruffled conformation for Ni^{II}tTETPP cannot be due solely to packing forces and the possibility remains that multiple conformations may exist, including a yet unidentified saddle conformation for Ni^{II}tTETPP. Such a case has been described for Ni^{II}DPP, where ruf, wave, and saddle conformations have been identified in different crystalline modifications and derivatives.[11c]

Overall, the structures of the Cu(II) complexes are very similar to those of the respective Ni(II) complexes. Selected structural data and a comparison with Cu^{II}TPP,[24] Cu^{II}OEP,[25] and Cu^{II}OETPP[8] are given in Tables 3 and 4. All Cu(II) complexes exhibited significant degrees of ruffling in addition to the saddle distortion mode (see Figure 2 and C_m displacements in Table 3). Individual differences are found in the degree of macrocycle distortion, which is generally 10−30% smaller than that found in the Ni(II) complexes. Interestingly, Cu^{II}tTETPP did not crystallize in a completely ruffled conformation as did Ni^{II}tTETPP but rather retained an overall saddle-shaped distortion like the other compounds. On the basis of the ordering of the UV/vis data, a similar conformation is assumed to be

(23) (a) Meyer, E. F., Jr. *Acta Crystallogr.* **1972**, *B28*, 2162. (b) Cullen, D. L.; Meyer, E. F., Jr. *J. Am. Chem. Soc.* **1974**, *96*, 2095. (c) Alden, R. G.; Crawford, B. A.; Doolen, R.; Ondrias, M. R.; Shelnutt, J. A. *J. Am. Chem. Soc.* **1989**, *111*, 2070. (d) Brennan, T. D.; Scheidt, W. R.; Shelnutt, J. A. *J. Am. Chem. Soc.* **1988**, *110*, 3919.

(24) Fleischer, E. B.; Miller, C. K.; Webb, L. E. *J. Am. Chem. Soc.* **1964**, *86*, 2342.

(25) Pak, R.; Scheidt, W. R. *Acta Crystallogr.* **1991**, *C47*, 431.

Table 6. Selected Bond Lengths (Å) and Angles (deg) for the Nickel(II) Porphyrins Studied

					Ni^{II}tTETPP[b]				
	quadrant	Ni^{II}OEP, tricl[a,23b]	Ni^{II}OEP, tetr[23a]	Ni^{II}DETPP	mol 1	mol 2	Ni^{II}cTETPP	Ni^{II}HETPP	Ni^{II}OETPP[a,9]
$N-C_a$	N21	1.376(4)	1.386(2)	1.394(9)	1.394(10)	1.396(9)	1.388(5)	1.391(5)	1.381(2)
	N22		*c*	1.385(9)	1.381(10)	1.377(9)	1.386(5)	1.384(6)	
	N23		*c*	1.396(9)	*c*	*c*	1.383(5)	1.384(5)	
	N24		*c*	1.382(9)	*c*	*c*	1.384(5)	1.382(5)	
C_a-C_b	N21	1.443(3)	1.449(5)	1.444(10)	1.450(11)	1.462(10)	1.456(6)	1.450(6)	1.451(3)
	N22		*c*	1.430(10)	1.441(11)	1.446(10)	1.456(6)	1.461(6)	
	N23		*c*	1.429(10)	*c*	*c*	1.432(6)	1.459(6)	
	N24		*c*	1.440(10)	*c*	*c*	1.433(5	1.435(6)	
C_b-C_b	N21	1.346(2)	1.362(5)	1.365(10)	1.378(11)	1.359(11)	1.361(6)	1.371(6)	1.365(5)
	N22		*c*	1.342(10)	1.344(11)	1.344(11)	1.353(6)	1.365(6)	
	N23		*c*	1.343(10)	*c*	*c*	1.344(6)	1.364(6)	
	N24		*c*	1.359(10)	*c*	*c*	1.349(6)	1.352(6)	
C_a-C_m	N21	1.371(4)	1.372(2)	1.398(10)	1.401(10)	1.388(11)	1.394(6)	1.394(6)	1.395(2)
	N22		*c*	1.397(10)	1.400(11)	1.383(11)	1.396(6)	1.400(6)	
	N23		*c*	1.392(10)	*c*	*c*	1.393(6)	1.398(6)	
	N24		*c*	1.389(10)	*c*	*c*	1.393(5)	1.387(6)	
N−M−N	adj	90.2(1)	90.0	90.2(2)	90.0(2)	90.1(2)	90.4(1)	90.5(2)	90.6(2)
N−M−N	opp	180.0	180.0	172.9(3)	178.7(5)	175.1(4)	170.0(1)	169.7(2)	168.7(1)
$M-N-C_a$	N21	128.0(2)	127.4(2)	126.3(5)	127.1(5)	126.2(5)	125.8(3)	126.0(3)	125.3(2)
	N22		*c*	126.8(5)	126.8(5)	126.5(5)	126.5(3)	126.3(3)	
	N23		*c*	127.5(5)	*c*	*c*	127.2(3)	126.4(3)	
	N24		*c*	126.5(5)	*c*	*c*	127.3(3)	126.9(3)	
C_a-N-C_a	N21	103.9(2)	105.1(3)	104.8(6)	105.6(6)	106.2(6)	105.9(3)	105.4(3)	105.9(2)
	N22		*c*	104.8(6)	106.2(6)	106.2(6)	105.2(3)	105.4(3)	
	N23		*c*	103.7(6)	*c*	*c*	104.7(3)	105.3(3)	
	N24		*c*	105.3(6)	*c*	*c*	104.9(3)	105.2(3)	
$N-C_a-C_b$	N21	111.6(3)	110.6(2)	110.3(6)	110.3(6)	109.3(6)	109.6(4)	110.1(3)	109.8(1)
	N22		*c*	110.2(6)	109.5(6)	109.6(6)	110.0(4)	110.2(3)	
	N23		*c*	110.7(6)	*c*	*c*	110.4(4)	110.3(4)	
	N24		*c*	110.3(6)	*c*	*c*	110.3(3)	110.2(4)	
$C_a-C_b-C_b$	N21	106.5(3)	106.8(3)	107.6(5)	106.7(6)	107.3(6)	107.1(4)	106.9(4)	106.8(1)
	N22		*c*	107.3(6)	107.5(7)	107.3(6)	107.1(4)	106.7(4)	
	N23		*c*	107.4(6)	*c*	*c*	107.2(4)	106.7(4)	
	N24		*c*	106.4(6)	*c*	*c*	107.1(4)	107.1(4)	
$N-C_a-C_m$	N21	124.4(3)	124.0(2)	121.8(7)	123.0(6)	122.7(6)	122.5(4)	122.2(4)	121.3(2)
	N22		*c*	123.6(6)	125.5(7)	124.3(7)	121.9(4)	122.2(4)	
	N23		*c*	123.4(6)	*c*	*c*	124.4(4)	122.4(4)	
	N24		*c*	125.4(6)	*c*	*c*	124.0(0)	124.2(4)	
$C_a-C_m-C_a$	N21	125.1(3)	124.1(2)	121.7(6)	119.5(7)	122.1(7)	122.3(9)	122.5(4)	121.4(1)
	N22		*c*	122.0(6)	121.6(7)	120.1(7)	121.9(4)	121.6(4)	
	N23		*c*	120.6(6)	*c*	*c*	121.9(4)	121.8(4)	
	N24		*c*	121.7(6)	*c*	*c*	121.6(4)	122.0(4)	
$C_m-C_a-C_b$	N21	124.1(3)	125.0(2)	127.5(6)	125.9(7)	127.6(7)	127.5(4)	127.5(4)	128.3(1)
	N22		*c*	125.6(6)	124.3(7)	125.5(7)	127.7(4)	127.1(4)	
	N23		*c*	125.6(6)	*c*	*c*	124.7(4)	126.8(4)	
	N24		*c*	124.4(6)	*c*	*c*	125.1(4)	123.4(4)	

[a] Average data for geometrically equivalent positions. [b] Two crystallographically independent molecules. [c] Generated by symmetry operation.

predominant in solution, and thus the view of Cu^{II}tTETPP given in Figure 2 might be taken as an indication for the conformation of a putative saddle-shaped Ni^{II}tTETPP.

The zinc(II) porphyrins again gave results similar to those described for the free bases or Ni(II) or Cu(II) complexes. Selected structural data are compiled in Tables 3, 4, and 7 and compared with data for Zn^{II}TPP,[26] Zn^{II}OEP(pyr),[27] and Zn^{II}-OETPP(MeOH).[7] However, zinc(II) has the propensity to form five-coordinated species with donor molecules, and depending on the crystallization conditions, different axial ligands are present in the individual compounds. Thus, two crystal structures were obtained for Zn^{II}DETPP, one with an axial methanol and the other with β-picoline as the axial ligand. Considerable differences were observed between these two forms (Figure 2). While the conformation of the methanol adduct resembled that found for the corresponding free base, the β-picoline adduct showed significantly larger deviations from planarity for the pyrrole rings with N22 and N24 and had a considerable degree of ruffling mixed into the conformation. Since neither methanol nor β-picoline is a sterically demanding axial ligand, the differences between both structures may be taken as a measure of the flexibility inherent in the DETPP macrocycle. Similar results were observed for the Zn^{II}(pyridine) complexes of tTETTP and cTETPP. Notably, Zn^{II}tTETPP(pyr) exhibited the only β-ethyl-substituted pyrrole ring (N21) in the present series, which deviated less from the mean plane than a β-H-substituted pyrrole (e.g., N22). However, the axial pyridine was severely disordered, and thus results for this compound have to be interpreted with some caution.

Zn^{II}HETPP could be crystallized both as the four-coordinate compound Zn^{II}HETPP without any axial ligand and as the five-coordinate complex Zn^{II}HETPP(pyr) with an axial pyridine.

(26) (a) Golder, A. J.; Povey, D. C.; Silver, J.; Jassim, Q. A. A. *Acta Crystallogr.* **1990**, *C46*, 1210. (b) Scheidt, W. R.; Mondal, J. U.; Eigenbrot, C. W.; Adler, A.; Radonovich, L. J.; Hoard, J. L. *Inorg. Chem.* **1986**, *25*, 795.

(27) Cullen, D. L.; Meyer, E. F., Jr. *Acta Crystallogr.* **1976**, *B32*, 2259.

(28) Medforth, C. J.; Senge, M. O.; Forsyth, T. P.; Hobbs, J. D.; Shelnutt, J. A.; Smith, K. M. *Inorg. Chem.* **1994**, *33*, 3865. Senge, M. O.; Medforth, C. J.; Forsyth, T. P.; Lee, D. A.; Olmstead, M. M.; Jentzen, W.; Pandey, R. K.; Shelnutt, J. A.; Smith, K. M. *Inorg. Chem.* **1997**, *36*, 1149.

Table 7. Selected Bond Lengths (Å) and Angles (deg) for the Zinc(II) Porphyrins

	quadrant	Zn^{II}OEP (pyr)[a,27]	Zn^{II}TPP, tricl[a,26b]	Zn^{II}DETPP (MeOH)	Zn^{II}DETPP (β-pic)	Zn^{II}tTETPP (pyr)	Zn^{II}cTETPP (pyr)	Zn^{II}HETPP	Zn^{II}HETPP (pyr)	Zn^{II}OETPP (MeOH)[a,7]
$N-C_a$	N21	1.366(1)	1.376(2)	1.376(8)	1.377(6)	1.376(5)	1.377(5)	1.376(7)	1.370(4)	1.371(4)
	N22			1.370(8)	1.372(6)	1.377(5)	1.377(4)	1.382(7)	1.378(4)	
	N23		*b*	1.371(8)	1.370(6)	1.373(5)	1.373(5)	1.375(7)	1.371(4)	
	N24		*b*	1.373(8)	1.377(6)	1.370(5)	1.374(5)	1.381(7)	1.379(4)	
C_a-C_b	N21	1.452(6)	1.440(3)	1.465(9)	1.458(6)	1.462(6)	1.451(5)	1.465(8)	1.458(5)	1.461(2)
	N22			1.434(9)	1.434(7)	1.442(6)	1.467(5)	1.453(9)	1.460(5)	
	N23		*b*	1.442(9)	1.443(7)	1.462(6)	1.444(5)	1.468(6)	1.464(5)	
	N24		*b*	1.446(9)	1.431(7)	1.445(6)	1.445(5)	1.438(7)	1.446(5)	
C_b-C_b	N21	1.353(5)	1.349(3)	1.369(9)	1.364(7)	1.364(6)	1.366(5)	1.379(8)	1.370(5)	1.370(7)
	N22			1.345(9)	1.341(7)	1.352(6)	1.365(5)	1.384(7)	1.371(5)	
	N23		*b*	1.343(9)	1.343(7)	1.367(6)	1.357(5)	1.364(8)	1.370(5)	
	N24		*b*	1.346(9)	1.332(7)	1.349(6)	1.349(5)	1.366(7)	1.351(5)	
C_a-C_m	N21	1.390(6)	1.400(3)	1.413(9)	1.406(6)	1.410(6)	1.418(5)	1.412(8)	1.410(5)	1.416(3)
	N22			1.418(9)	1.407(7)	1.405(6)	1.414(5)	1.415(7)	1.414(5)	
	N23		*b*	1.403(9)	1.405(7)	1.409(6)	1.408(5)	1.405(7)	1.414(5)	
	N24		*b*	1.401(9)	1.412(7)	1.405(6)	1.404(5)	1.408(7)	1.407(5)	
N−M−N	adj	88.8(1)	90.0(1)	89.4(2)	88.6(2)	88.7(1)	88.7(1)	90.1(2)	88.4(1)	89.4(4)
N−M−N	opp	163.0(16)	180.0(1)	168.5(2)	162.0(2)	162.7(1)	162.1(1)	174.7(2)	160.4(1)	167.8(4)
$M-N-C_a$	N21	126.7(3)	126.4(1)	126.7(4)	125.1(3)	125.3(3)	123.2(2)	124.2(3)	123.0(2)	122.9(6)
	N22			126.5(4)	126.7(3)	126.3(3)	126.0(2)	124.6(3)	125.5(2)	
	N23		*b*	126.6(4)	126.1(3)	123.8(3)	126.1(2)	124.8(4)	122.8(2)	
	N24		*b*	126.5(4)	126.9(3)	126.4(3)	126.5(2)	126.6(4)	126.5(2)	
C_a-N-C_a	N21	106.4(5)	106.6(2)	106.7(5)	107.0(4)	107.2(3)	106.8(3)	107.6(4)	107.1(3)	107.7(5)
	N22			106.3(5)	106.5(4)	107.2(3)	106.9(3)	106.6(5)	107.3(3)	
	N23		*b*	106.6(5)	106.7(4)	107.0(3)	106.7(3)	107.8(4)	107.4(3)	
	N24		*b*	106.7(5)	106.2(4)	107.2(3)	107.0(3)	106.1(4)	106.8(3)	
$N-C_a-C_b$	N21	110.1(4)	109.4(2)	110.0(5)	109.4(4)	109.4(4)	109.5(3)	109.4(5)	109.6(3)	109.2(3)
	N22			109.7(5)	109.3(4)	108.9(4)	109.7(3)	109.8(4)	109.3(3)	
	N23		*b*	109.4(5)	109.4(4)	109.7(4)	109.6(3)	108.9(5)	109.4(3)	
	N24		*b*	109.4(6)	109.2(4)	109.2(4)	109.1(3)	109.8(4)	109.2(3)	
$C_a-C_b-C_b$	N21	106.7(2)	107.4(2)	106.2(6)	106.9(4)	106.9(4)	106.9(3)	106.7(5)	106.6(3)	106.8(2)
	N22			107.2(6)	107.4(4)	107.5(4)	106.8(3)	106.7(6)	106.9(3)	
	N23		*b*	107.3(6)	107.3(4)	106.7(4)	107.0(3)	107.0(4)	106.7(3)	
	N24		*b*	107.2(6)	107.7(4)	107.3(4)	107.3(4)	107.0(4)	107.4(3)	
$N-C_a-C_m$	N21	124.3(5)	125.9(2)	123.6(6)	123.4(4)	123.2(4)	122.6(3)	123.1(5)	121.9(3)	122.4(2)
	N22			126.4(6)	126.1(4)	126.1(4)	123.6(3)	122.3(5)	123.2(3)	
	N23		*b*	125.1(6)	125.0(4)	123.3(4)	124.7(3)	123.2(4)	122.5(3)	
	N24		*b*	126.5(6)	125.8(4)	126.2(4)	125.8(3)	124.6(4)	125.7(3)	
$C_a-C_m-C_a$	N21	127.9(3)	124.8(2)	125.1(6)	125.3(4)	125.1(4)	126.4(3)	124.9(4)	125.3(3)	124.4(4)
	N22			125.5(6)	124.9(4)	125.3(4)	125.1(3)	124.9(5)	125.1(3)	
	N23		*b*	124.8(6)	125.5(4)	124.9(4)	124.8(4)	124.7(4)	124.3(3)	
	N24		*b*	127.2(6)	125.7(4)	126.4(4)	124.6(3)	123.8(5)	124.7(3)	
$C_m-C_a-C_b$	N21	125.5(3)	124.6(2)	126.4(6)	127.1(4)	127.4(4)	127.8(3)	127.5(5)	128.3(3)	128.2(2)
	N22			123.8(6)	124.6(4)	125.0(4)	126.7(3)	127.6(5)	127.5(3)	
	N23		*b*	125.5(6)	125.5(4)	127.1(4)	125.4(4)	127.9(5)	128.1(3)	
	N24		*b*	124.0(6)	124.9(4)	124.6(4)	125.0(4)	125.3(5)	125.0(3)	

[a] Average values for geometrically equivalent positions. [b] Generated by symmetry operation.

Differences between both compounds in bond lengths and angles for the metal centers are typical for the four- and five-coordinated zinc(II) porphyrins. The four-coordinated complex showed slightly larger overall deviations from planarity and exhibited more pronounced differences between substituted and unsubstituted pyrrole rings. The differences between the four- and five-coordinated Zn^{II}HETPP were considerably smaller than those between the two Zn^{II}DETPP structures. Displacements of the zinc(II) center from the N_4 plane and structural data for the axial ligands of all five-coordinated porphyrins (Table 4) were comparable to those found for other five-coordinated zinc(II) porphyrins.[14]

In addition to asymmetric distortion modes being induced by the peripheral substituent pattern, some degree of asymmetry is also induced by the axial ligand. In all five-coordinated species described here, the degree of macrocycle distortion was less for the macrocycle side facing the axial ligand than for other. This can be exemplified by comparing the N21 and N23 quadrants (which face toward the axial ligand) with those of N22 and N24 (which point away from the axial ligand) in Table 3.

For symmetric, highly nonplanar metalloporphyrins, it has been established that the size of the central metal is inversely correlated to the degree of macrocycle distortion.[8,12b] Thus, for a given macrocycle system, the overall degree of nonplanarity should decrease in the order Ni(II) > Cu(II) > Zn(II). Table 3 shows that this order is retained at every level of β-ethyl substitution, i.e. at every level of inherent steric strain. For example, the Δ24 values are 0.62, 0.55, and 0.50 Å for Ni^{II}OETPP, Cu^{II}OETPP, and Zn^{II}OETPP, respectively. A similar ordering of 0.49, 0.44, and 0.33 Å for M = Ni, Cu, and Zn, respectively, is observed for M^{II}cTETPP. This effect is retained when individual quadrants of the porphyrin system are inspected, and all data indicate that, with respect to structural data like out-of-plane displacements or changes in bond lengths and angles,[8] metal effects in asymmetric saddle-distorted porphyrins are similar to those found for symmetric porphyrins.

Conclusions

The data presented here indicate that mixed condensation of pyrrole, diethylpyrrole, and benzaldehyde yields a series of porphyrins which show successively more nonplanar macro-

cycles in the order TPP < DETPP < tTETPP < cTETPP < HETPP < OETPP. Crystal structures reveal that the increasing steric strain imposed on the macrocycle by introduction of successively more β-ethyl groups remains to some extent localized in the respective regions of the porphyrin macrocycle. Thus, asymmetric saddle-shaped distortions of the macrocycle are observed for most compounds. Observation of the ruffled Ni^{II}tTETPP is another example of the inherent flexibility of the porphyrin macrocycle. Preliminary data[29] show this series to be an excellent candidate for further spectroscopic and photophysical studies, which will be reported in due course.

Acknowledgment. This work was supported by grants from the Fonds der Chemischen Industrie and the Deutsche Forschungsgemeinschaft (Se543/2-4 and Heisenberg-Stipendium Se543/3-1). We are indebted to Prof. Smith for his continuing support and for providing instrument time at the UC Davis crystallographic facility and to Drs. K. M. Barkigia and J. Fajer (Brookhaven National Laboratory) for providing the crystallographic coordinates for H_2OETPP.

Supporting Information Available: Figures showing the atom numbering, thermal ellipsoid plots, and deviations of the macrocycle atoms from planarity for all compounds, selected packing plots and side views of individual molecules, and tables listing the core size, bond lengths, and bond angles for the Cu(II) porphyrins, phenyl tilt angles, and packing analyses (37 pages). Ordering information is given on any current masthead page. The results of the crystal structure determinations have been deposited with the CCDC.

(29) Büchner, M.; Röder, B. Personal communication.

IC970765G